



**HAL**  
open science

## Recent advances in layered double hydroxide /polymer latexes nanocomposites: from assembly to in situ formation.

V. Prévot, Elodie Bourgeat-Lami

### ► To cite this version:

V. Prévot, Elodie Bourgeat-Lami. Recent advances in layered double hydroxide /polymer latexes nanocomposites: from assembly to in situ formation.. Layered Double Hydroxide Polymer Nanocomposites. 1st Edition, pp.461, 2019, 10.1016/B978-0-08-101903-0.00012-4 . hal-02394389

**HAL Id: hal-02394389**

**<https://hal.science/hal-02394389>**

Submitted on 4 Dec 2019

**HAL** is a multi-disciplinary open access archive for the deposit and dissemination of scientific research documents, whether they are published or not. The documents may come from teaching and research institutions in France or abroad, or from public or private research centers.

L'archive ouverte pluridisciplinaire **HAL**, est destinée au dépôt et à la diffusion de documents scientifiques de niveau recherche, publiés ou non, émanant des établissements d'enseignement et de recherche français ou étrangers, des laboratoires publics ou privés.

# **Recent advances in layered double hydroxide /polymer latexes nanocomposites: from assembly to *in situ* formation.**

V. Prevot<sup>1</sup> and E. Bourgeat-Lami<sup>2</sup>

<sup>1</sup> Université Clermont Auvergne, CNRS, ICCF - Institut de Chimie de Clermont-Ferrand, F-63000 Clermont-Ferrand, France. <sup>2</sup> Univ Lyon, Université Claude Bernard Lyon 1, CPE Lyon, CNRS, UMR 5265, Chemistry, Catalysis, Polymers and Processes (C2P2), 43 Bvd. Du 11 Nov. 1918, F-69616 Villeurbanne, France.

**Abstract.** In this chapter, recent advances in the synthesis of waterborne LDH/polymer nanocomposites by using LDH and/or latexes as building blocks of self-assembled materials are reviewed. Three main routes can be distinguished: electrostatic assembly of preformed LDH particles with oppositely charged latex particles, *in-situ* polymerization involving the formation of polymer latexes in the presence of LDH particles, and latex-templating which consists in LDH synthesis at the latex surface or confined in a polymeric colloid crystal used in this case as sacrificial template. The mechanical and flame retardancy properties of the resulting LDH nanocomposites are reviewed, providing insight into the main requirements of LDH fillers with respect to various applications. The performance of LDH macroporous structures as a function of their porosity is also discussed.

**Keywords:** Layered Double Hydroxides, Latex, Emulsion polymerization, Macroporosity, Inverse opals

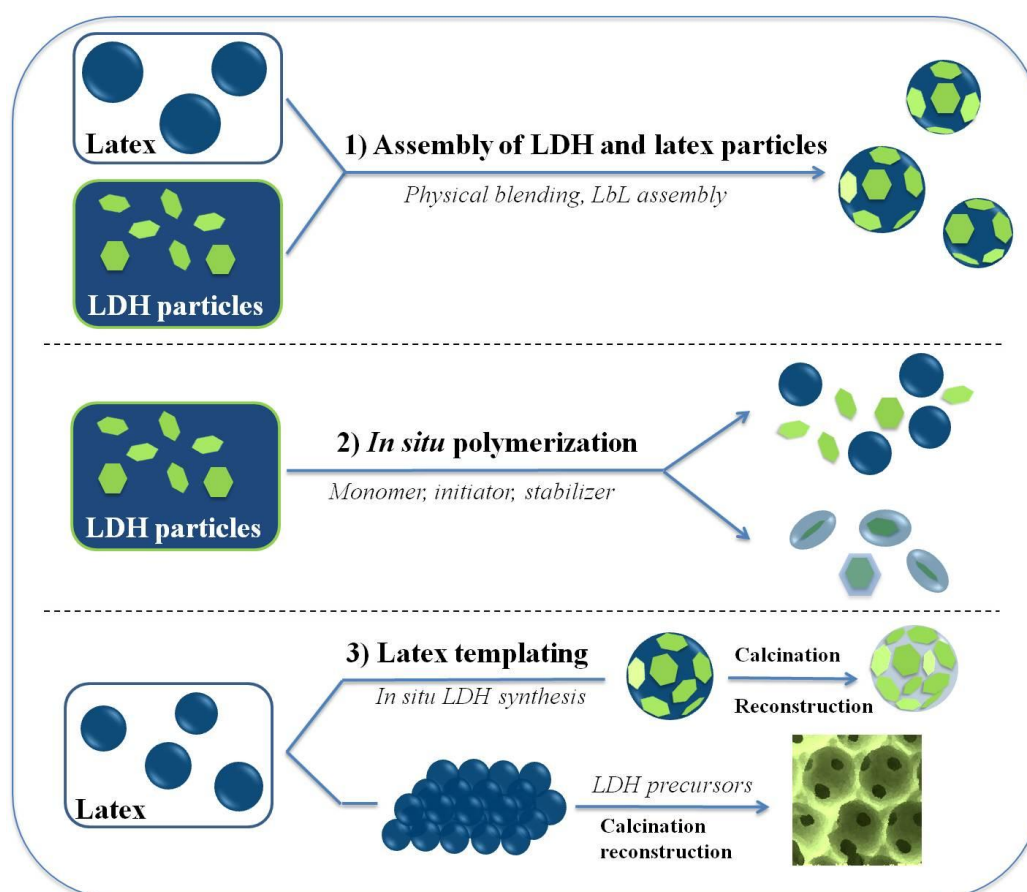
## 1- Introduction

In the past two decades, there has been considerable interest in the development of polymer nanocomposite systems for various applications.<sup>1</sup> Some of the reported benefits of nanocomposite formation are improved barrier properties, scratch resistance, hardness/toughness and fire resistance. In the case of clay particles, one of their main interests is their ability to exfoliate or intercalate in the presence of polymer chains, allowing enhanced performances at very low filler loadings. It is generally accepted that clay exfoliation (rather than intercalation) favors the performance improvement, especially for mechanical reinforcement and barrier properties.<sup>2</sup> The benefits of exfoliated clay layers result from the many interactions between the polymer and the nanoclay layers, strengthening and reinforcing the polymer system, and yet being sufficiently small that the particles have no effect on the visual properties of the coating. The improved barrier performance is generally thought to arise from an increase in the tortuous path distance for water to reach the substrate, and this effect can be - and is - achieved by using lamellar platelets. Compared with the well-established use of 2D fillers from the smectite group such as montmorillonite (MT),<sup>3</sup> preparing layered double hydroxides (LDHs)/polymer nanocomposites has only recently attracted considerable attention due to the peculiar physical and chemical properties of LDHs.<sup>4</sup> Because of their anion exchange properties, LDHs are also often referred to as 'anionic clays'. LDHs display many interesting features such as wide-ranging chemical compositions, variable layer charge densities, ion-exchange properties, reactive interlayer spaces and hydroxylated surfaces. The structure of hydrotalcite - one of the most studied minerals of the LDH family - is related to that of brucite,  $Mg(OH)_2$  in which a portion of the  $Mg^{2+}$  has been replaced by  $Al^{3+}$ . Carbonate anions (along with water) are intercalated between the layers to maintain electroneutrality. The hydrotalcite chemical formula is therefore given

as  $\text{Mg}_{0.75}\text{Al}_{0.25}(\text{OH})_2(\text{CO}_3)_{0.125} \cdot 0.5\text{H}_2\text{O}$ . Based on a combination of a large variety of divalent and trivalent metal cations, the general formula for the LDH family can be written as  $(\text{M}^{\text{II}}_{1-x}\text{M}^{\text{III}}_x(\text{OH})_2)(\text{A}^{\text{m-}}_{x/m} \cdot n\text{H}_2\text{O})$  where  $(\text{M}^{\text{II}}_{1-x}\text{M}^{\text{III}}_x(\text{OH})_2)$  represents the layer, and  $(\text{A}^{\text{m-}}_{x/m} \cdot n\text{H}_2\text{O})$  represents the interlayer species. LDHs are not naturally abundant, however synthetic LDH phases can be easily prepared in a large quantity and organically modified.<sup>5</sup> LDH particles size can be tuned over a large range with lateral dimensions ranging from 30 nm<sup>6</sup> to more than 5  $\mu\text{m}$ <sup>7</sup> and thicknesses from 1 nm to 20 nm. The high aspect ratios are of interest for enhancing mechanical properties and permeability in nanocomposites. Moreover, the anion exchange capacity can be tuned from 200 to 450 meq/100 g by varying the proportion of trivalent metal cation. Such high values induce strong electrostatic cohesion between the stacked layers and the interlayer species which limits swelling in water but does not hamper exfoliation under specific conditions, especially during polymer nanocomposites preparation.<sup>8</sup> As for other types of nanofillers, most studies have focused on the inclusion of LDHs into solvent-borne formulations and much less attention has been dedicated to waterborne processes. In most cases, it is the desired nature of the polymer matrix that determines the choice of synthesis method. Typically, in presence of water-insoluble monomers and/or polymers, organically-modified LDHs are incorporated in the nanocomposite by melt intercalation, organic solution intercalation, exfoliation/adsorption or *in situ* polymerization, while water-soluble polymeric species allow pristine LDHs to be directly intercalated in water. Emulsion and suspension polymerization are important alternatives for producing polymeric particles and nanocomposites in water from water-insoluble monomers.<sup>10</sup> The synthesis of polymer/LDH nanocomposites by emulsion and suspension polymerization has been recently addressed by Qiu and Qu<sup>9</sup> in a comprehensive review covering the different synthetic pathways for preparing LDH/polymer nanocomposites, their properties and potential applications. However, the use of post-synthetic assembly techniques and the synthesis of

LDH macroporous structures using latex particles as colloidal templates was not covered in this review

The present review chapter intends to present the current-state of the art in the synthesis of waterborne LDH-based nanocomposites and macroporous LDH materials using latex technology. Special attention will be paid to the interactions involved at the nanoscale level between the polymeric species and the inorganic LDH matrices, since these are crucial for determining the properties of the final nanocomposites. Three main strategies will be distinguished: assembly of preformed LDH and latex particles, *in situ* polymerization and latex-templating (Scheme 1).



**Scheme 1.** Scheme illustrating the three main routes to LDH-based nanocomposites and macroporous materials by latex technology: a) assembly of preformed LDH and latex particles, b) *in situ* polymerization and c) latex-templating.

In the first approach, the self-assembly process is promoted by electrostatic interactions between the LDH and latex particles. Interfacial interactions and particles size thus play a key role in determining the morphology of the resulting nanocomposites. The second strategy relies on the *in situ* formation of polymer latexes in the presence of LDH particles using emulsion or suspension polymerization. Conversely, the third strategy is a templating approach in which LDH synthesis is performed at the latex surface or confined in a polymeric colloid crystal, giving macroporous materials with enhanced diffusion pathways and reactivities. Finally, the last part is devoted to the main properties of the resulting LDH nanocomposites, particularly mechanical and flame retardancy properties, and the applications in which LDH macroporous structures have played an important role.

## **2- Use of latex technology for the production of LDH-based composite materials and macroporous structures**

The possibility to associate latex technology and LDH inorganic building blocks has been investigated only recently compared to other nanocomposite preparation methods. This is mainly due to the specific properties of LDH such as poor swelling in water and highly stacked layered structures, limiting their efficient use in waterborne processes. However, recent advances in the synthesis of LDH nanosheets with tunable particle dimensions, exfoliation properties and improved colloidal stability has enabled the development of new approaches. Waterborne processes permit the design of both LDH structured nanocomposites and LDH-based porous materials. Regardless of the method used, controlling the LDH/polymer interfacial properties is key to achieving the desired morphology and performance of the hybrid materials. The three main routes depicted above are detailed in the

following sections and for each of them, some key aspects and associated challenges are highlighted.

## 2.1 Assembly of preformed LDH and latex particles

### 2.1.1 Layer-by-layer assembly

Since Decher and co workers<sup>11</sup> demonstrated in 1997 that uniform polymer films could be deposited onto mineral substrates by the sequential adsorption of polyanions and polycations using the so-called layer-by-layer (LbL) assembly technique, interest in polyelectrolyte assembly has increased considerably. Over the past twenty years, this technique has evolved into a versatile and scalable tool for colloidal and surface engineering. In brief, the LbL technique relies on the adsorption of a polyelectrolyte onto an oppositely charged surface (typically a solid substrate or a colloid), removing the excess polyions by rinsing, and repeating the procedure sequentially with oppositely charged polyelectrolyte. Charge overcompensation occurs after every adsorption step, which allows adsorption of the subsequent oppositely charged layers. The LbL approach was used for the preparation of thin films involving polyelectrolyte/LDH multilayers on 2D substrates,<sup>12</sup> but there has been much less work done on the synthesis of LDH/latex composite materials by the LbL approach. Li et al.<sup>13</sup> reported the formation of core-shell particles by alternate deposition of Mg-Al LDH nanosheets and poly(sodium 4-styrene sulfonate) (PSSNa) (up to 20 layer pairs in total) onto polystyrene (PS) beads ( $D_p = 1.3 \mu\text{m}$ ) (Figure 2a-b). Hollow capsules were subsequently obtained after removal of the PS core and the PSS polyanion by calcination at 500 °C (Figure 1c-d). A slow heating ( $< 1 \text{ }^\circ\text{C min}^{-1}$ ) was key to preserving the core-shell morphology. The crystalline LDH structure was destroyed upon heating but was recovered after 12 h exposure

to humid air (Figure 1e-f) as attested by high-resolution transmission electron microscopy (HR-TEM) (Figure 1g) and wide-angle X-ray diffraction (XRD) (Figure 1h) analyses.

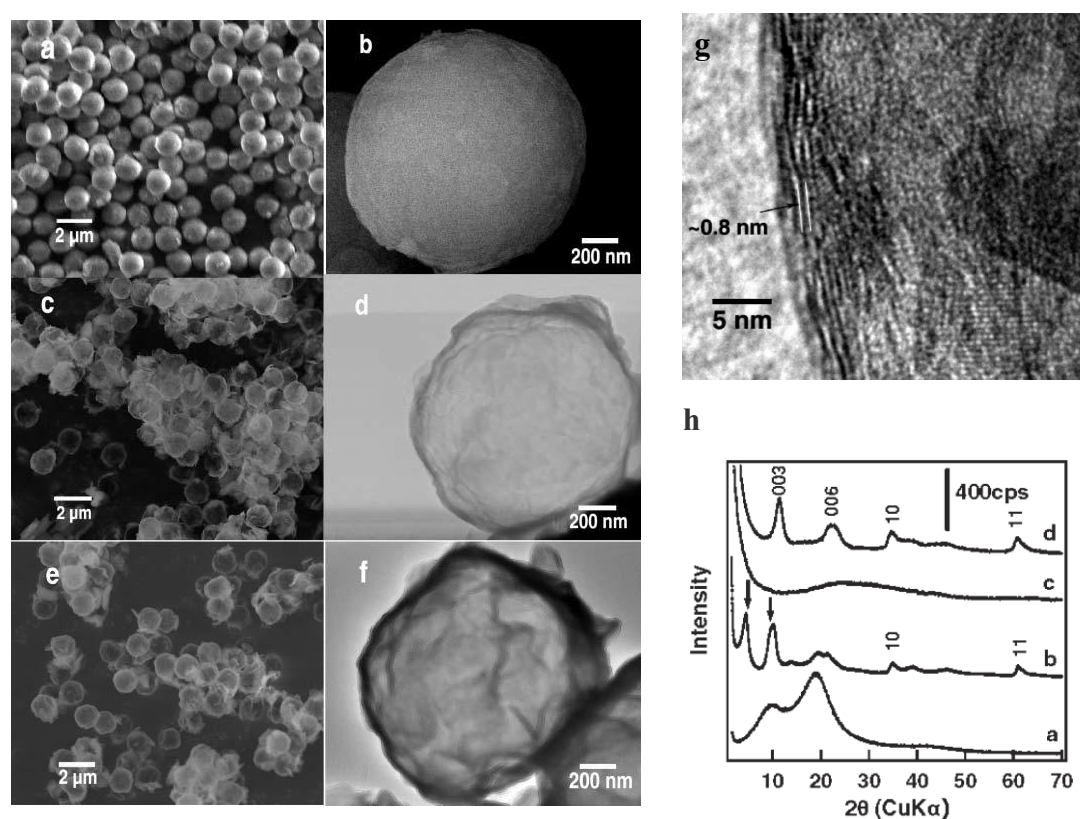


**Figure 1.** Scanning and transmission electron microscopy images of core-shell particles (a, b) and LDH capsules (c, d) obtained by LbL assembly followed by calcination of the colloidal template and reconstruction of the LDH crystalline structure by exposition to humid air (e, f). HR-TEM (g) and XRD (h) were used to confirm the crystalline LDH structure. Reproduced from ref. <sup>13</sup> Copyright 2017 The Royal Society of Chemistry.

Another example of LbL assembly was reported by Bujdoso et al.<sup>14</sup> In this work, sulfonated PS latex particles with 55 and 560 nm average diameters were first prepared and doped with silver particles through the adsorption of silver salts and subsequent reduction by sodium borohydride. A multilayer film was then grown on a glass substrate by deposition of the negatively charged PS@Ag particles and Mg/Al LDH platelets. Surface plasmon resonance

and atomic force microscopy were used to monitor the growth process and determine the thickness of the LbL films. The films made from the large particles were heterogeneous and contained a high amount of free silver nanoparticles, whereas those obtained from the small particles were more regular. Optical measurements revealed that the thickness of the LDH/PS<sub>560</sub>@Ag films was built up mainly from the silver nanoparticles. As expected, the films obtained from the smaller particles displayed lower roughness values. The resulting hybrid films are of potential interest as antibacterial surfaces.

### 2.1.2 Physical blending

The production of nanocomposites through physical blending of a polymer latex with inorganic particles such as carbon nanotubes,<sup>15</sup> few-layer graphene,<sup>16</sup> graphene oxide or silica<sup>17</sup> particles has been already reported by several authors and is a rather straightforward process. In the case of 2D objects, a segregated network is formed by confining the plate-like fillers in the interstices between the latex particles during the drying process.<sup>18</sup> To secure the final segregated network morphology, self-assembly strategies have been reported that aim at promoting interactions between the latex and LDH particles during film formation. As LDH possesses a high positive surface charge in a large range of pH values, electrostatic interaction is often used to secure the cellular morphology. For instance, Veschambres et al.<sup>19</sup> reported LDH-based nanocomposite films obtained by casting a mixture of LDH platelets (30-140 nm in lateral size) and oppositely-charged poly(methyl methacrylate-*co*-*n*-butyl acrylate) [P(MMA-*co*-BA)] latex particles (700 nm in diameter). The self-assembly process was driven by mutual electrostatic interaction between the positively charged platelets and the latex beads leading to the formation of a 3D nanostructure as illustrated in Figure 2.

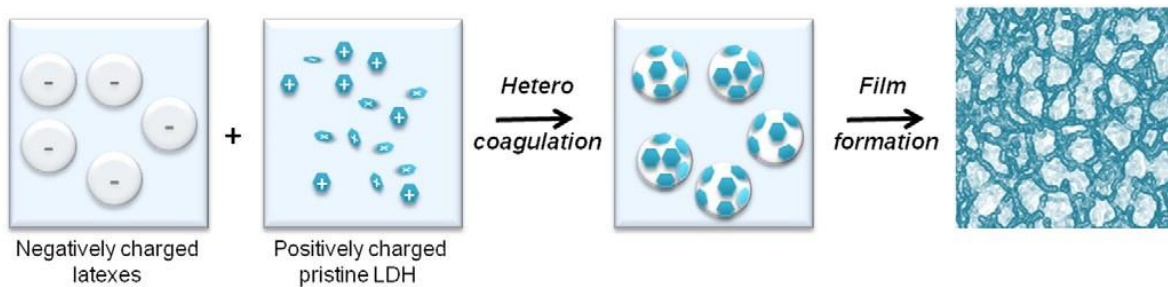


**Figure 2.** Scheme illustrating electrostatic self-assembly of LDH platelets with oppositely-charged P(MMA-co-BA) latex particles and the subsequent formation of a nanocomposite film with honeycomb-like 3D microstructure. Reproduced from ref. <sup>19</sup> with permission from Elsevier.

Several parameters can influence the self-assembly behavior and the microstructure of the hybrid films. The size ratio between the LDH lateral size and the latex bead diameter is clearly an important parameter, as it determines the morphology of the clay network and the mesh size. Maintaining the colloidal stability of these binary systems is also critical to forming homogeneous films. Indeed, aggregation of the latex-LDH composites may lead to the formation of irregularly shaped clusters and to rough surfaces during coating. The mechanism of interaction between polymer latex particles and oppositely charged LDH platelets and its effect on the colloidal stability of the binary mixture, was studied in detail by Pavlovic et al. <sup>20</sup> The authors used electrophoretic mobility and time-resolved dynamic light scattering measurements to estimate the surface charge density and the stability ratio of the binary suspensions. Fast aggregation occurred for intermediate clay concentrations due to the neutralization of the negative surface charges of the polymer particles while stable suspensions were obtained for high and low LDH doses (Figure 3a). The electrophoretic mobility increased with increasing LDH concentration due to their adsorption on the oppositely charged latex surface. Charge neutralization occurred at the isoelectric point, where the overall charge of the particles was zero, while further increase of the LDH dose led

to charge inversion (Figure 3c). TEM observation of the resulting composite suspensions revealed that the polymer spheres were completely coated with the clay platelets once the inorganic concentration was sufficiently high (Figure 3b).

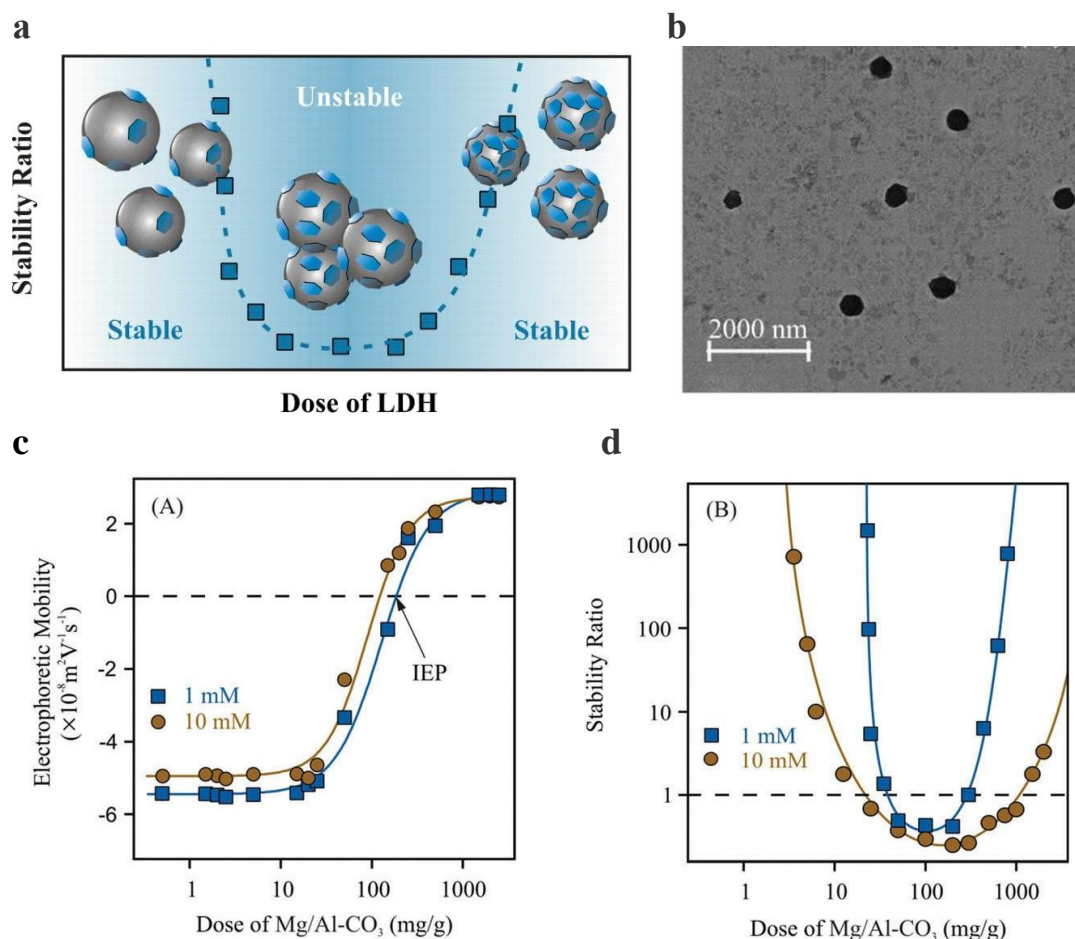


**Figure 3.** Scheme illustrating the mechanism of charging and aggregation of LDH/latex binary suspensions obtained by mixing stable colloidal suspensions of oppositely charged Mg/Al-CO<sub>3</sub> LDH platelets and P(MMA-co-BA) latex particles (40 mg L<sup>-1</sup>) at pH 9 for different ionic strengths. a) Schematic representation of the aggregation mechanism as a function of the LDH dose, b) TEM image for the highest LDH dose (1000 mg g<sup>-1</sup>) where the latex underwent charge inversion, c) electrophoretic mobility and d) stability ratio values. Reproduced from ref.<sup>20</sup> with permission from The Royal Society of Chemistry.

The obtained results, and in particular the influence of ionic strength on the stability ratios, indicated that the aggregation behavior of the suspensions could be satisfactorily described by the classical Derjaguin, Landau, Verwey and Overbeek (DLVO) theory with the contribution of two opposing interparticle forces: van der Waals attraction and electrostatic double layer repulsion. Interestingly, an additional attractive Coulomb interaction between positively charged LDH patches on the particle surface and negatively charged empty places on another approaching latex particles, was also identified.

The question of dispersion stability was also addressed by Braga et al.<sup>21</sup> during the preparation of nitrile rubber (NR)/LDH composites by latex blending and coagulation. Pluronic F-127 was used as dispersing agent together with ultrasound in order to decrease the size of the clay agglomerates in water and promote the formation of stable suspensions. Steric repulsion between the NR and LDH particles enabled homogeneous dispersion of the clay platelets in the NR matrix. During the drying process, with the evaporation of water, the viscosity increased, fixing likewise the LDH plates in the system while heat curing crosslinked the different NR particles together. Although XRD did not show any effect of Pluronic F-127 on clay exfoliation, field emission gun scanning electron microscopy (FE-SEM) revealed that the LDH particles were more homogeneously dispersed in the matrix when the surfactant was used.

## 2.2 LDH-based nanocomposites by *in situ* emulsion and suspension polymerizations

*In situ* polymerization consists in performing the polymerization reaction in the presence of the filler material. In the *in situ* intercalative polymerization method pioneered by Toyota,<sup>22</sup> the layered silicate is swollen with a liquid monomer (or eventually a monomer solution), and the polymerization occurs between the intercalated clay layers. The synthesis of

nanocomposites via *in situ* emulsion or suspension polymerization proceeds according to a fundamentally different mechanism due to the multiphasic nature of the polymerization medium. In order to facilitate understanding of the following discussion, the specific features of these two polymerization processes are briefly described below before giving detailed examples illustrating the potential of these techniques for the production of LDH-based nanocomposites.

### 2.2.1 Conventional emulsion polymerization

Emulsion polymerization allows the synthesis of stable aqueous colloidal dispersions of polymer particles, known as latexes.<sup>23</sup> In “conventional” emulsion polymerization, the polymer particles are formed by starting from an insoluble (or scarcely soluble) monomer emulsified by the aid of a surfactant above its critical micellar concentration. The monomer is originally distributed between coarse emulsion droplets, surfactant micelles and the water phase where a small proportion of monomer (depending on its solubility) is molecularly dissolved. The initiator is soluble in water and polymerization thus starts in the aqueous phase by the formation of radicals through the initiator thermolysis and the addition of the first monomer units. The formed oligoradicals are captured by the monomer-swollen micelles where the polymerization continues, leading to solid particles. The growth of particles proceeds by diffusion of monomer from the monomer droplets, through the aqueous phase, into the growing particles. Emulsion polymerization is very versatile and allows tuning of the particle morphology and composition (e.g., formation of core-shell particles and other equilibrium morphologies) by successive additions of different monomers. Compared to bulk or solution polymerization, emulsion polymerization offers significant advantages such as

better control of heat and viscosity of the medium, and the possibility of increasing the molecular weight of the polymer chains without affecting the rate of polymerization.

Over the last twenty years, emulsion polymerization has proven highly suitable for the production of polymer/inorganic particles.<sup>10</sup> In particular, there has been a large body of experimental work on the incorporation of smectite clays (mainly Laponite and MT) into polymer latexes.<sup>24</sup> In contrast, the amount of scientific publications reporting the synthesis of LDH-based composite latexes by emulsion polymerization can be brought down to a few papers. One main reason is that, as mentioned earlier, LDHs have poor swelling properties in water. To circumvent this issue, Chen et al.<sup>25</sup> reported an all *in situ* approach wherein LDH platelets are formed at the same time as the latex particles. The composite material was obtained by adding an aqueous solution of sodium hydroxide to an emulsion consisting of magnesium and aluminum metal salts, methyl methacrylate as a monomer, sodium dodecyl sulfate (SDS) as surfactant and benzoyl peroxide (BPO) as a thermal initiator, and increasing the temperature to 80 °C to start polymerization. The authors reported that *in situ* intercalation of DS anions allowed the polymerization to proceed in the clay galleries, resulting in intercalated PMMA chains. Unfortunately, since the latex suspension was unstable, no information was given at that time on particle morphology. The main advantage of the *in situ* approach however, is that the LDH platelets are well dispersed in the polymer matrix leading to transparent composites even for high clay loadings (up to 50 wt%). Ding et al.<sup>26</sup> used a very similar approach to synthesize exfoliated PS/ZnAl LDH. The SDS surfactant was replaced by N-lauroyl-glutamate (LG), while *n*-hexadecane was used to promote clay exfoliation (Figure 4). XRD confirmed the successful formation of the LDH platelets. Again as the latex was precipitated before characterization, there was no information about latex stability and morphology. In a subsequent paper from the same group,<sup>27</sup> the nature of the

surfactant and the presence of *n*-hexadecane were shown to be key to the obtention of a fully exfoliated morphology.

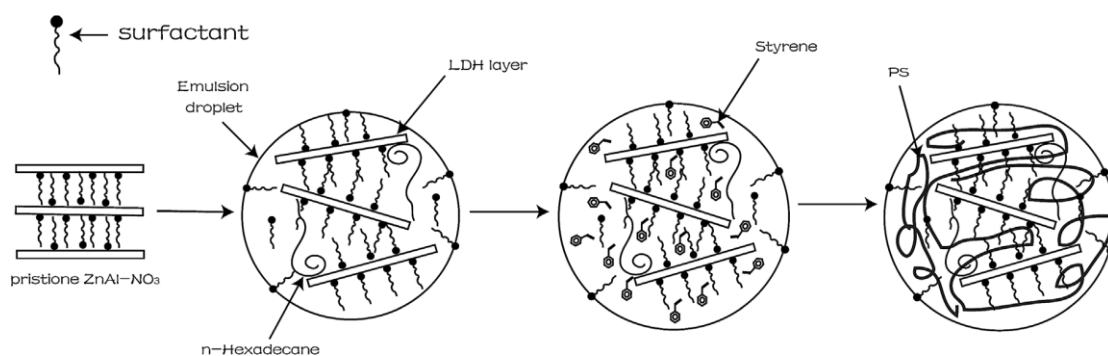


**Figure 4.** Scheme illustrating the possible mechanism of formation of exfoliated PS/LDH nanocomposites via all *in situ* LDH and latex synthesis by emulsion polymerization of styrene in the presence of *n*-hexadecane. Reproduced from ref. <sup>26</sup> with permission from Elsevier.

The authors studied the thermal properties of the resulting materials and showed that the thermal decomposition temperature of the PS/LDH nanocomposites was comparable to that of the PS matrix for low clay contents but decreased with increasing clay contents. This was associated with the presence of LG, which decomposed in the range 180–320 °C. To prevent the drawback of the presence of a surfactant, Qiu et al. <sup>28</sup> prepared PS/LDH composites via surfactant-free emulsion polymerization using KPS as thermal initiator. XRD was used to monitor the changes of the interlayer spacing throughout the course of the reaction, and revealed successful intercalation of the persulfate initiator anions in between the LDH layers. As the polymerization progressed, the intercalated S<sub>2</sub>O<sub>8</sub><sup>2-</sup> ions as well as the initiator molecules in solution formed oligomers which entered the clay galleries and further enlarged the interlayer space leading to a fully exfoliated PS/LDH nanocomposite at the end of the reaction as confirmed by TEM and XRD analyses. The precise location of the clay (i.e., either inside or outside the latex particles), however, could not be determined from the TEM images.

Quite a few authors have also used organically modified LDHs. For instance, Zhao et al.<sup>22a</sup> reported the preparation of Mg-Al-LDH intercalated by dodecyl sulfate (DS) anions through the co-precipitation method, and their subsequent incorporation into poly (*n*-butyl acrylate-*co*-vinyl acetate) (P(BA-*co*-VAc) latexes by emulsion polymerization using KPS as initiator and poly(vinyl alcohol) (PVA) as stabilizer. A pre-emulsion was firstly formed by dispersing part of the monomer suspension containing the DS-intercalated LDH platelets in a water solution of PVA, and polymerized by slow addition of the initiator solution. The rest of the monomer and clay was then introduced in the reactor and the polymerization was continued until complete monomer-to-polymer conversion. The final latex was recovered by filtration and cast into films, and unfortunately again no information was given on particle size and morphology, the emphasis being placed instead on the thermal and flame-retardant properties of the resulting materials (see section 3.1.2, below). In the same vein, Kovanda et al.<sup>29</sup> reported the co-intercalation of DS and various monomeric anions ((meth)acrylates, 4-vinyl benzoate and 2-acrylamido-2-methyl-1-propanesulfonate) into Mg-Al-NO<sub>3</sub> and Zn-Al-NO<sub>3</sub> LDHs, either by ion exchange or by direct co-precipitation. The intercalated LDHs were used for the preparation of poly(butyl methacrylate) (PBMA)/LDH nanocomposites through *in situ* emulsion polymerization. The overall procedure was very similar to the one of Zhao et al. The organoclay was first suspended in the monomer (BMA) and the mixture was pre-emulsified in water using SDS as surfactant. Part of the pre-emulsion (around 5 wt%) was polymerized at 85 °C for 10 minutes using ammonium persulfate as initiator and the remaining part was fed in the reactor together with the initiator solution at a constant rate, slow enough to ensure starved conditions. The polymerization was finally pursued for 30 minutes leading to a latex suspension of around 30% solids content. Compared to DS-intercalated LDHs, the additional presence of a reactive monomer in the clay galleries promoted clay exfoliation by *in situ* formation of polymer chains as schematically represented in Figure 5a. However, compared

to solution polymerization, *in situ* emulsion polymerization resulted in a poorer dispersion state of the LDH platelets within the PBMA matrix as attested by the higher slope value in the small angle X-ray scattering (SAXS) experiments (Figure 5b).

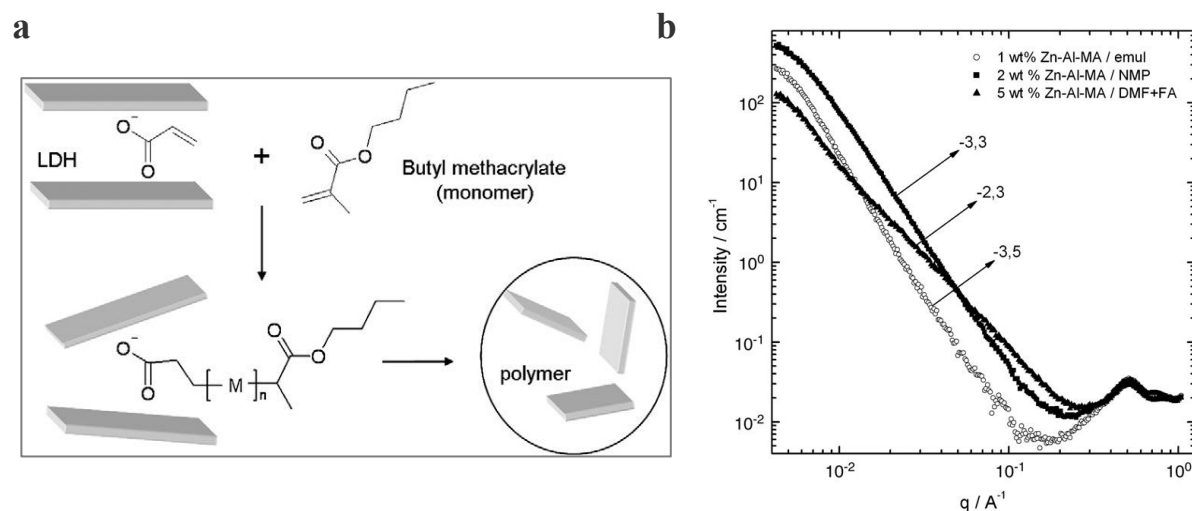


**Figure 5.** a) Scheme of LDH/PBMA nanocomposite formation by *in situ* starve-feed emulsion polymerization of BMA using LDH with intercalated monomeric and DS anions, and b) SAXS patterns of PBMA films containing Zn–Al-MA LDHs prepared by emulsion polymerization or by solution polymerization in 1-methyl-2-pyrrolidone (NMP) or in a mixture of dimethylformamide and formamide (DMF+FA). Reproduced from ref. <sup>29</sup> with permission from Elsevier.

### 2.2.2 Suspension polymerization

Suspension polymerization can be roughly described as a bulk polymerization in which the monomer containing dissolved organosoluble initiator molecules is suspended as droplets in the aqueous continuous phase. Droplets of the organic phase are formed and maintained in suspension by the use of: (i) vigorous agitation throughout the reaction and (ii) hydrophilic macromolecular stabilizers dissolved in water (e.g. low molar mass polymers such as PVA, polyvinylpyrrolidone or hydroxymethylcellulose). Each droplet thus acts as a small bulk

polymerization reactor to which the normal kinetics apply. Polymer is produced in the form of beads whose average diameter is close to that of the initial monomer droplets (0.01 to 2 mm). The resulting polymer beads are easily isolated by filtration provided they are rigid and not tacky. Therefore, suspension polymerization is unsuitable for preparing polymers that have low glass transition temperatures, but is widely used for styrene, methyl methacrylate or vinyl chloride monomers for instance.

To our best knowledge, there are only two articles reporting the synthesis of polymer/LDH nanocomposites by suspension polymerization.<sup>27, 30</sup> Ding et al.<sup>27</sup> used a very similar all *in situ* approach as that described above for emulsion polymerization, where the water-soluble initiator was simply replaced by an oil soluble initiator, and actually obtained poorer results and in particular lower clay exfoliation. However, strictly speaking, the process cannot be considered as a true suspension polymerization as a surfactant was used to stabilize the resulting particles. Bao et al.<sup>30</sup> reported the synthesis of poly(vinyl chloride)/LDH composite resins by *in situ* suspension polymerization of vinyl chloride monomer (VCM) using diethylhexyl peroxydicarbonate as radical initiator and PVA as suspending agent. The LDH particles were first intercalated by DS anions and then dispersed in VCM followed by vigorous stirring at room temperature to promote the formation of an homogeneous clay dispersion. The polymerization was initiated by increasing the temperature to 57 °C. The resulting composite products were recovered by filtration and dried at 60°C prior to characterization. The polymerization performed in the presence of DS-LDH led to smaller particles than pure PVC, suggesting that the LDH platelets contributed to the stabilization of the polymer beads. TEM revealed a partially exfoliated/ partially intercalated morphology and a better dispersion state than composite materials obtained by direct melt-blending, showing the superiority of the *in situ* approach for the synthesis of PVDC/LDH nanocomposites.

### 2.2.3 Reversible deactivation radical polymerization (RDRP)

Reversible deactivation radical polymerization (formally known as controlled/living radical polymerization – CRLP) refers a family of polymerization techniques enabling the synthesis of well-defined macromolecular architectures. RDRP processes are based on the reversible deactivation of propagating radicals, either through a reversible termination mechanism [e.g., nitroxide-mediated polymerization (NMP) or atom transfer radical polymerization (ATRP)] or reversible chain transfer [reversible addition fragmentation chain transfer (RAFT)] reaction. The rapid equilibrium between active propagating radicals and dormant species ensures that all chains have an equal opportunity to propagate, which gives narrow molar mass distributions. RDRP does not only allow the preparation of polymers with well-defined molar mass, dispersity, end group functionality, topology and architecture (e.g., block, stars, combs, etc), but also offers unprecedented opportunities in materials design, including the ability to prepare organic/inorganic nanocomposites and surface tethered (co)polymers. The growth of polymer chains from inorganic surfaces is a topic of considerable interest and the reader is referred to a number of recent comprehensive reviews for an in-depth description of the various synthetic strategies.<sup>31, 32, 33, 34, 35</sup> A wide variety of inorganic substrates have been investigated including cationic clays (such as MT or Laponite<sup>36</sup>) and LDHs. In particular, various authors have shown that it is possible to grow polymer chains directly from the surface of LDH particles using either ATRP<sup>37, 38</sup> or RAFT<sup>39, 40</sup> polymerization providing access to exfoliated polymer/LDH nanocomposites. However, those polymerizations were performed in bulk or in solution, and are therefore beyond the scope of this review. RDRP can also be conducted in water solution and an extensive range of water-soluble or water-insoluble monomers can nowadays be polymerized using aqueous controlled radical polymerization methods.<sup>41</sup> The transposition of RDRP techniques to dispersed polymerization

systems (i.e., emulsion polymerization and other related heterophase processes) is however not straightforward and significant effort has been devoted in the last ten years to implement RDRP in aqueous dispersed media.<sup>41</sup> One important recent development in the field is polymerization induced self-assembly (PISA) which is a special case of emulsion polymerization based on the *self-assembly* of *in situ* generated block copolymers. Briefly, the PISA process involves chain extending a hydrophilic polymer precursor prepared via RDRP with hydrophobic monomer(s) to form amphiphilic chains which self-assemble into spherical nano-objects or more complex morphologies depending on reaction conditions. The notable advantages of this process are the absence of low molecular weight surfactant in the suspension, the possibility to polymerize a wide range of monomers, and to form a variety of morphologies at high solids content without the aid of an organic co-solvent. A few years ago, the approach was extended to the encapsulation of inorganic particles<sup>42, 41, 43</sup> recognizing that most of the hydrophilic polymer precursors used in the PISA process are also capable of interacting with inorganic compounds. Although there have been a few examples involving NMP<sup>44</sup> and ATRP,<sup>45</sup> most work in this field has used RAFT polymerization. In short, the method, coined RAFT-assisted encapsulating emulsion polymerization (REEP), consists of the adsorption of a pre-prepared living amphiphilic random copolymer (hereafter denoted macroRAFT agent) on the surface of the inorganic particles, followed by emulsion polymerization of a hydrophobic monomer. Following this method, Cenacchi et al.<sup>46</sup> demonstrated very recently the first example of LDH encapsulation by REEP. A random copolymer of acrylic acid (AA) and BA [P(AA<sub>17</sub>-*stat*-BA<sub>17</sub>)] was first synthesized by RAFT polymerization, and then electrostatically adsorbed on Mg<sub>2</sub>Al-LDH particles to provide both colloidal stability and reactivatable groups from which the subsequent emulsion polymerization could proceed, leading to LDH encapsulation. Both nitrate and carbonate-intercalated LDHs were investigated, showing noticeable differences between the two

precursors. The nitrate-intercalated LDH showed higher adsorption capacity than its carbonate counterpart because interlayer nitrate ions (in addition to those on the outer surface) were also displaced by the macroRAFT agent. The two macroRAFT agent-modified LDHs were then engaged in the emulsion polymerization of methyl acrylate (MA) and BA (MA/BA 80/20 wt/wt) using 2,2'-azobis(2-methylpropionamide)dihydrochloride (AIBA) or 2,2'-azobis(N,N'-dimethylene-isobutyramidine)dihydrochloride (ADIBA) as radical initiators. Regardless the type of LDH and initiator, cryo-TEM showed successful encapsulation of the LDH nanoplatelets in the core of the latex particles (Figure 6).

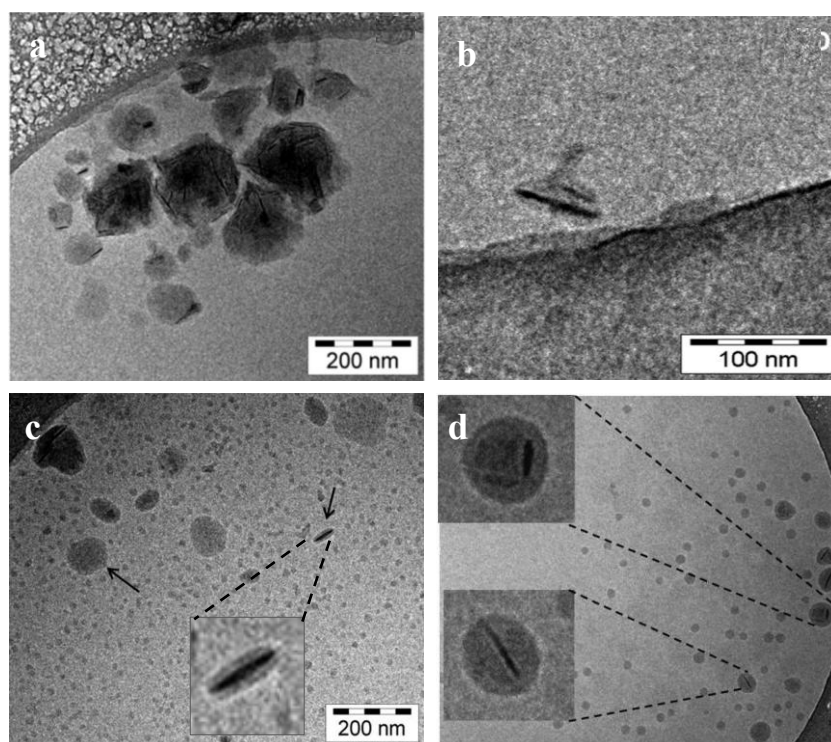


**Figure 6.** Cryo-TEM images of the final P(MA-*co*-BA)/LDH nanocomposite particles obtained by REEP using : a, b) Mg<sub>2</sub>Al-NO<sub>3</sub> and c, d) Mg<sub>2</sub>Al-CO<sub>3</sub>-LDH with [macroRAFT] = 3 mmol L<sup>-1</sup>, MA/BA (80/20 wt/wt), pH = 8.0, T = 70 °C and initiator = AIBA (a-c) or ADIBA (d). In b), the initial macroRAFT/LDH suspension was sonicated for 5 minutes before polymerization. The arrows point to individually-encapsulated LDH platelets. Reproduced from ref. <sup>46</sup> with permission from The Royal Society of Chemistry.

The nitrate produced however near-spherical isotropic nanocomposite latexes with several LDH platelets per particle (Figure 6a), whereas the carbonate led to monoencapsulation under the same conditions (Figure 6c). This was attributed to different initial dispersion states of the LDH-modified precursors. Indeed, elongated core-shell particles containing a single encapsulated LDH platelet were also obtained when the macroRAFT-modified nitrate LDH was submitted to an ultrasonic treatment prior to REEP (Figure 6b). All polymerizations displayed limited conversions, which was attributed to the poor hydrolytic stability of AIBA. The conversion effectively increased when AIBA was replaced by ADIBA – an initiator known to be less sensitive to hydrolysis - which also resulted in more spherical particles due to the higher amount of polymer formed around each clay platelet.

### 2.3 Latex-templating approaches

Inorganic particles associated with latex particles are not only interesting in polymer science to produce polymer nanocomposite materials but also to design nanostructured materials. In this latter case, the polymer beads are no longer the main component of interest, but are instead considered as a ‘sacrificial hard template’ allowing the precursor solutions or particles to either coat the template surface or fill the voids (Figure 7). The polymer beads are subsequently removed either by calcination or dissolution to introduce the porosity and generate nanostructured macroporous materials. Uniform polystyrene beads are probably the most common colloidal particles used since their size can be easily tuned in a large range and they are commercially available. Monodisperse silica spheres have also been extensively used as sacrificial templates but are out of the scope of this chapter. Such synthetic strategies have been investigated to produce hollow capsules<sup>47</sup> and three dimensionally ordered macroporous structures (3DOM)<sup>48</sup> of various inorganic components including oxides and metals. In this

section, we summarize several recent examples which demonstrate the efficiency of the latex templating approach to produce nanostructured LDHs.

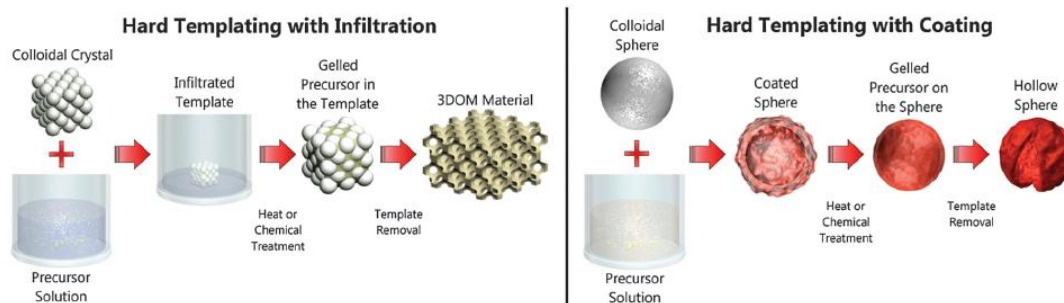


**Figure 7.** Schemes detailing the hard templating process. Left: An example of hard templating conducted using an infiltration process. Right: An example of hard templating conducted via a coating process. Reproduced from ref. <sup>48b</sup> with permission from The Royal Society of Chemistry.

As previously described in section 2.1, hollow capsules were prepared using the LbL technique at the surface of colloidal PS spheres.<sup>13</sup> Other synthetic methods have been described to produce LDH core-shell structures or hollow spheres using the latex templating approach. Du et al. reported on the possibility to directly perform LDH nucleation and growth on the surface of sulfonated PS-divinylbenzene cation-exchange resin beads ( $565 \pm 50 \mu\text{m}$ ).<sup>49</sup> To promote LDH nucleation, the beads were in a first step converted to a  $\text{Mg}^{2+}/\text{Al}^{3+}$  exchanged form and then added to a sodium hydroxide solution. The LDH growth was carried out by adding the metal salt solution, while the pH was kept constant at a value of 9. SEM images evidenced the formation of a LDH shell of 150 nm constructed from LDH platelets aligned edge-on in a monolayer (Figure 8). At longer reaction time, more LDH materials were deposited on the beads as a thick additional layer lying flat on the previous LDH shell.

However for this bead size, the supported LDH shell structure was not sufficiently stable to produce hollow LDH spheres by calcination, with the spheres collapsing upon heating.

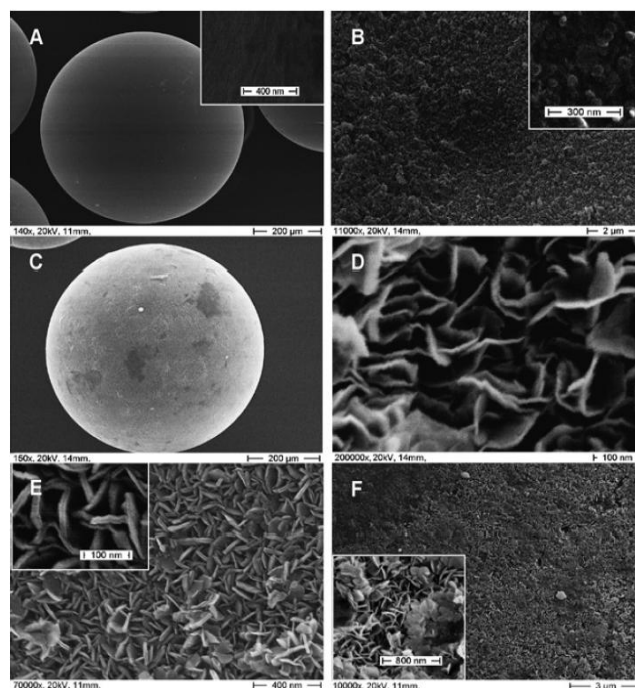


**Figure 8.** SEM images of (A) Mg<sup>2+</sup>/Al<sup>3+</sup>-exchanged polymer resin beads; (B) polymer beads recovered following exposure to NaNO<sub>3</sub>-NaOH solution for 1 h; (C, D) polymer beads recovered from the LDH synthesis reaction after 18 h; (E) polymer beads recovered from the LDH synthesis reaction after 30 h; (F) polymer beads recovered from the LDH synthesis reaction after 60 h. Reproduced from ref. <sup>49</sup> with permission from The Royal Society of Chemistry.

Similarly, negatively charged PS nanospheres (22-360 nm) were used as a hard template to produce MgAl@PS core shell particles by simple coprecipitation in the presence of the polymer spheres.<sup>50</sup> SEM images combined with EDS and XRD confirmed the LDH precipitation, which lead to a cracked appearance at the sphere surface. Interestingly, by tuning the rate of NaOH addition from 0.14 to 4.35 mL min<sup>-1</sup> during LDH coprecipitation in the presence of the PS spheres (0.6-1.6 μm) as the template, CoFe- LDH hollow spheres with

two different hierarchical morphologies were prepared.<sup>51</sup> Low addition rates resulted in a flower-like shell consisting of edge-on orientated LDH platelets, while high rates favored rapid nucleation to give raspberry-like morphologies with LDH nanoparticles oriented face-on to the PS bead surface (Figure 9). After calcination the flower-like morphology appeared close to collapsing, showing that the edge-on orientation is not favorable to the hollow sphere formation. Comparatively, the raspberry-like spheres maintained their morphology upon heating and LDH conversion in oxides and mixed oxides.

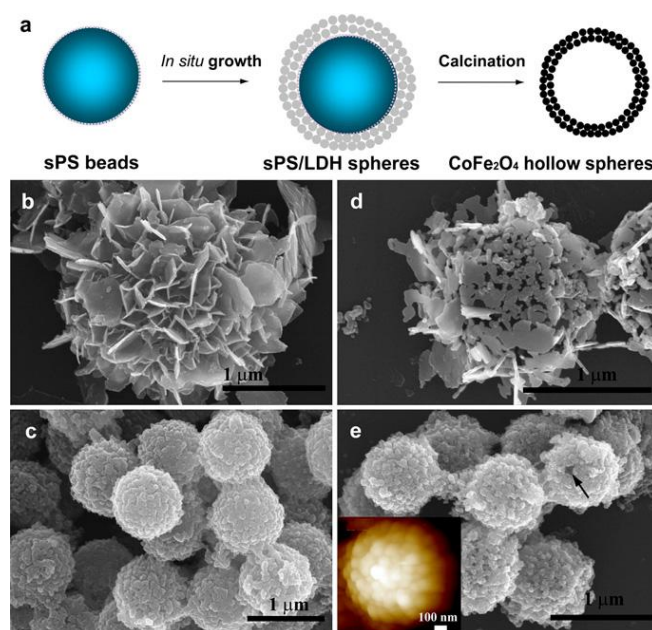


**Figure 9.** (a) Schematic illustration of the  $\text{Co}^{\text{II}}\text{Fe}^{\text{II}}\text{Fe}^{\text{III}}\text{-LDH}$  spherical shell formed on PS beads and the product obtained after its calcination in air. SEM images of (b) the flower-like  $\text{PS}/\text{Co}^{\text{II}}\text{Fe}^{\text{II}}\text{Fe}^{\text{III}}\text{-LDH}$  spheres obtained by slow addition of NaOH, (c) the raspberry-like  $\text{sPS}/\text{Co}^{\text{II}}\text{Fe}^{\text{II}}\text{Fe}^{\text{III}}\text{-LDH}$  spheres obtained by rapid addition of NaOH, (d)  $\text{CoFe}_2\text{O}_4$  porous spheres obtained by calcination of (b); and (e)  $\text{CoFe}_2\text{O}_4$  hollow spheres obtained by calcination of (c). A hole is marked with a black arrow in (e), and the inset of (e) shows an AFM image. Reproduced with permission from ref. <sup>51</sup>. Copyright 2017 Elsevier.

By direct coprecipitation in the presence of PS beads (350 nm) and a subsequent filtration step, macroporous MgAl LDH were obtained. The MgAl LDH coprecipitation was carried out into a PS colloidal solution by the addition of Mg and Al nitrate salts dissolved in a 1:1 water:ethanol solution and aqueous ammonia as precipitant.<sup>52</sup> Extended porous architectures were formed by a calcination/reconstruction process through agglomeration and fusion of nanocrystalline LDH platelets. A thin-walled honeycomb nanostructure was observed by SEM with macropores distributed throughout the materials in a non-ordered manner. Macroporous  $\text{CoFe}_2\text{O}_4$  spinel microspheres were also obtained by a simple process involving spray-drying of a suspension containing  $\text{CoFe}^{\text{II}}\text{Fe}^{\text{III}}$  LDH nanoparticles<sup>53</sup> (3.0 wt%) and sulfonated PS spheres (0.3 wt%).<sup>54</sup> The spinel phase was obtained by calcination at 700 °C of the  $\text{CoFe}^{\text{II}}\text{Fe}^{\text{III}}$  LDH/PS microspheres. The spherical morphology was retained upon heating leading to macroporous microspheres with a two-fold higher total pore volume ( $2.49 \text{ g cm}^{-1}$ ) than microspheres prepared without PS spheres.

Another latex-templating strategy relies on the use of a colloidal crystal to confine LDH nanoparticles and to subsequently produce three dimensionally ordered macroporous (3DOM) materials or inverse opals. This colloidal crystal templating method known to introduce well-ordered and interconnected pores into a material was recently deeply reviewed by A. Stein.<sup>48</sup> Geraud et al. were the first to demonstrate the possibility of confining LDH coprecipitation into the interstitial voids of a PS colloidal crystal template.<sup>55</sup> Typically, monodisperse negatively charged PS spheres were firstly assembled into close-packed face-centered cubic arrays by centrifugation forming millimeter to centimeter thick materials. Secondly, the LDH synthesis was carried out by coprecipitation using successive soaking of the well-organized colloidal crystal in a metal salt solution and (after a drying step) in sodium hydroxide. It is noteworthy that precursor solutions should be prepared using water/alcoholic mixture to ensure a good wettability of the PS colloidal crystal and precursor infiltration. Finally, 3DOM

LDH replicas were obtained either by template dissolution in toluene or using calcination/reconstruction. As shown in SEM images (Figure 10) the inorganic component formed an interconnected wall-type structure (wall thickness 60-110 nm), in which the windows interconnecting the pores are observed. Such interconnected macroporous networks promote more efficient diffusion through the macroporous material compared with materials obtained by stacking of core/shell spheres. Tilting TEM images in Figure 10 provided further evidence of the 3DOM structure. The different views of the pore array are consistent with views along the [111], [011], and [211] directions for replicas resulting from the fcc array.

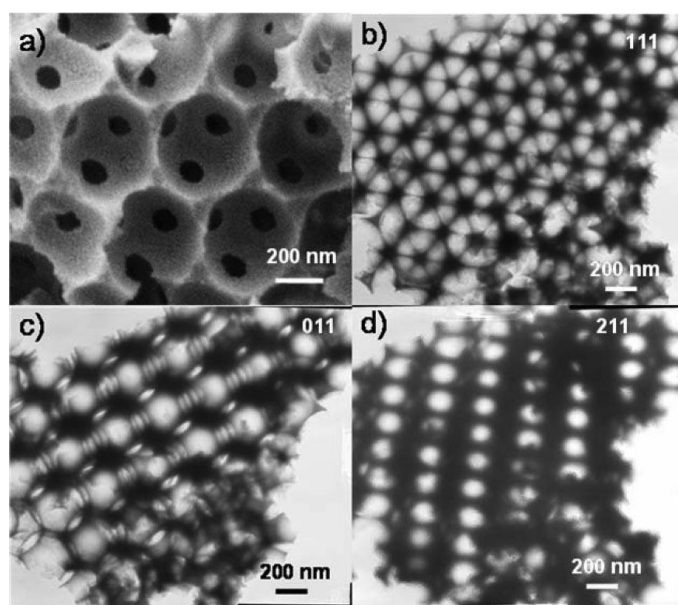


**Figure 10.** (a) SEM images of windows between macropores of NiAl matrix and three tilting TEM images showing the (b) [111], (c) [110], and (d) [211] directions (fcc lattice) of the macroporous NiAl LDH matrix. Reproduced with permission from ref. <sup>55b</sup>. Copyright 2017 American Chemical Society.

Obviously, the wetting interactions between the precursor and the template surface favored the formation of a coating following the curved surface, with giving relatively smooth walls. By modifying the diameter of the initial PS beads, the pore size was easily tuned from 280 nm

to 505 nm. This synthetic process was applied to a wide range of LDH layer compositions (MgAl, NiAl, CoAl, ZnAl, ZnCr, MgFeAl, MgCoAl, ...) and a large variety of anions was incorporated. Calcination in air at around 450 °C and 800 °C produced oxides and mixed oxide walls while maintaining the periodical structure. In parallel, a macroporous carbon replica was also successfully prepared by carbonization and demineralization from a 3DOM vinyl benzene sulfonate-intercalated MgAl LDH.<sup>56</sup>

Alternatively, NiAl LDH macroporous thin films were also successfully prepared on 2D substrates (tin-doped indium oxide (ITO), fluorine doped tin oxide (FTO) or platinum electrode) through the use of the inverse opal method and LDH electrodeposition.<sup>57</sup> In these cases, colloidal crystal was formed either by evaporation and capillary attractive forces or by electrophoresis at constant potential of 1.5 V for 30 s. Then, the PS bead (350–430 nm) coated slides were used as working electrodes for LDH electrosynthesis. LDH thin films can indeed be directly and easily electrosynthesized at an electrode surface<sup>58</sup> thanks to nitrate reduction, forming small, ill-crystallized LDH particles which homogeneously coat the electrode surface. Typically, the PS coated electrode was soaked in a Ni and Al salt solution (0.03 M) containing potassium nitrate (0.3 M) and NiAl LDH was cathodically deposited by applying a constant potential of -0.9 V. The removal of the PS array was done by extraction with solvent such as toluene or a mixture of tetrahydrofuran and acetone. The films were examined at different stages of deposition from 30 to 180 s. After 60 s of electrodeposition, a deposited layer 1200 nm thick was characterized. As illustrated by the SEM images (Figure 11), the LDH deposition in the interstices between the PS spheres was clearly seen, leading to a continuous LDH network surrounding interconnected cavities after PS dissolution.<sup>57</sup> Such electrochemically-induced precipitation of LDH appears more efficient for producing 2D macroporous thin films than the previously described successive impregnation method, which produced coating with numerous cracks, bare regions and over-coating.

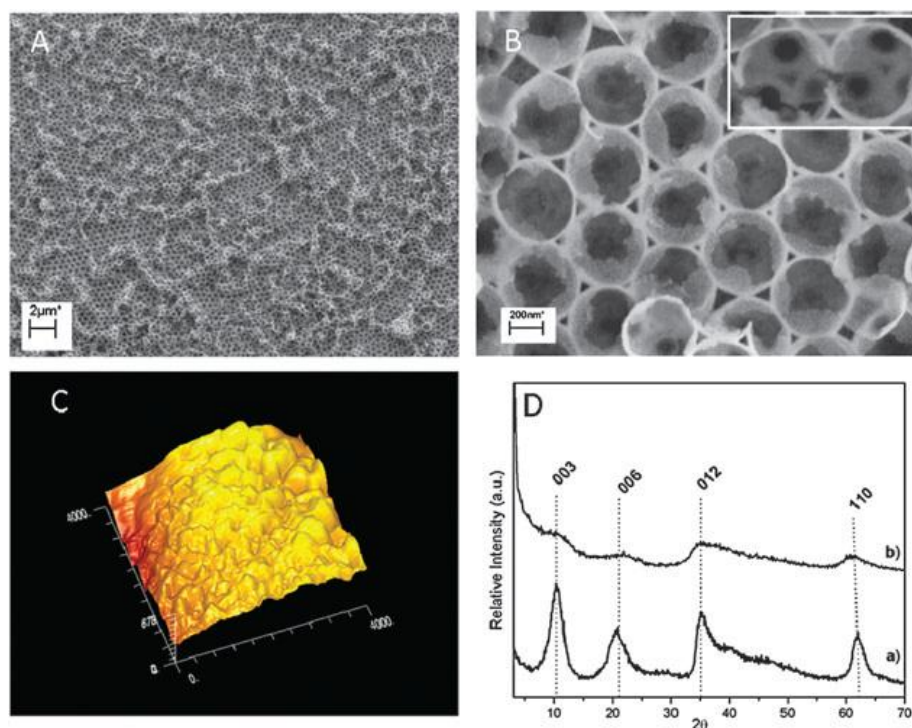


**Figure 11.** (A and B) FESEM images of NiAl 3D-OME (-0.9 V, 60 s) at different magnification, (C) the corresponding AFM image and (D) PXRD patterns of (a) coprecipitated NiAl LDH and (b) electrosynthesized NiAl LDH. Reproduced from ref. <sup>57a</sup> with permission from The Royal Society of Chemistry.

Still using a colloidal crystal template array, an alternative strategy has been employed to infiltrate a solution of LDH nanoclusters acting as colloidal building blocks.<sup>59</sup> The LDH nanoclusters were synthesized using a one-pot route involving acetylactone and propylene oxide in a mixture of ethanol and water (in addition to the metal salts). To prepare macroporous thin films, the diluted suspension of LDH nanoclusters was simply spin-coated on the PS (100 nm) array at 8000 rpm for 60 s and the polymer was chemically dissolved by chloroform. A well-defined macroporous thin film with a pore diameter of 80 nm was successfully obtained.

### **3- Properties of LDH-based nanocomposites and LDH macroporous structures**

#### 3.1 LDH-based nanocomposites

Fabrication of composites through the latex route has been widely used to produce clay-polymer composites with enhanced mechanical properties for high durability coatings, and with enhanced gas barrier properties for packaging applications. LDH platelets are good candidates to fulfill similar property enhancements. The following section describes the functional properties of materials formed from LDH-based nanocomposite latexes. The influence of physical properties and morphology of the precursor hybrid latexes on the final properties will be emphasized.

##### 3.1.1 Mechanical properties

Clays are well known as low cost fillers for thermoplastics and thermosets, imparting high modulus and tensile strength. It is generally accepted that the mechanical reinforcement of polymer/clay nanocomposites is due to the high aspect ratio and high surface area of the inorganic filler, and therefore requires the platelets to be well dispersed in the polymer matrix.<sup>2b</sup> A good clay dispersion also ensures optical transparency of the final material, which is a key aspect for coating applications. In addition, the establishment of clay-clay contacts and strong filler-filler interfacial interactions are known to be important requirements for good mechanical properties.<sup>60</sup> Recently, Veschambres et al.<sup>19</sup> studied the mechanical properties of LDH-based nanocomposite films obtained by casting a mixture of LDH platelets (30-140 nm in lateral size) and oppositely charged latex particles (700 nm in diameter). The films displayed a well-defined cellular microstructure, which induced a large mechanical

reinforcement significant of a mechanical percolation behavior (Figure 12a). As expected, the thickness of the network wall increased with increasing LDH content (Figure 12b) while focused ion beam (FIB)-SEM analysis suggested some alignment of the platelets in the film plane likely due to mechanical forces exerted on the clay network during film formation. Similar 3D morphologies have already been reported in the literature for smectite clays<sup>61, 62, 63</sup> but to our knowledge this is the first time that such a morphology is described for LDHs.

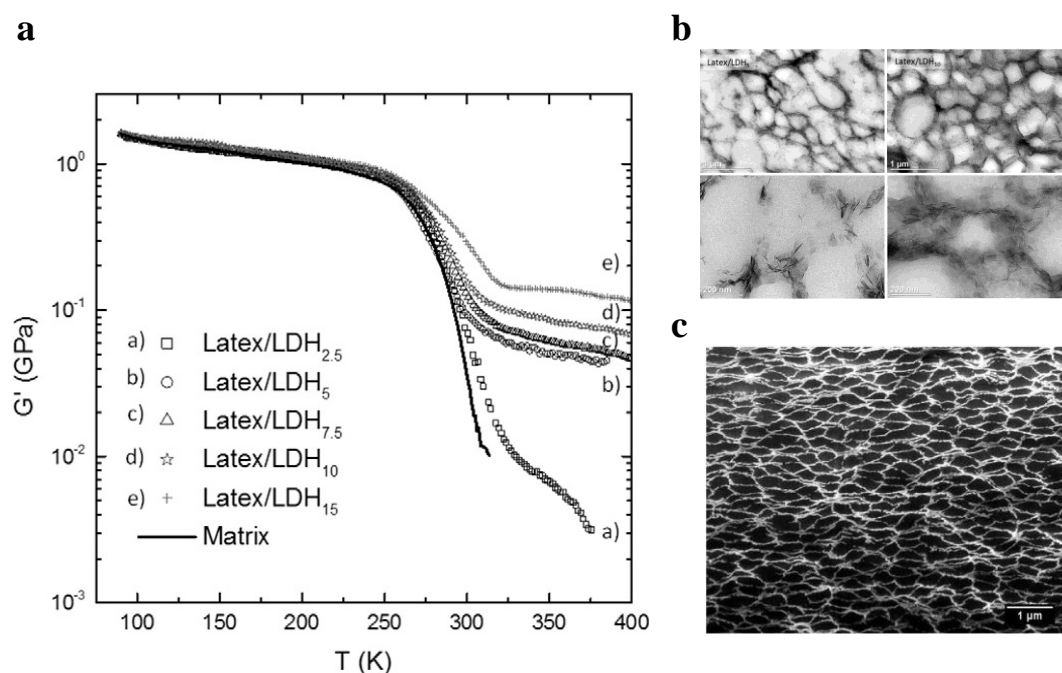


**Figure 12.** a) Effect of LDH volume fraction (based on polymer) on the mechanical properties of polymer/LDH nanocomposites films obtained by heterocoagulation of positively charged LDH layers and negatively charged latex particles and subsequent drying of the dispersions. b) Low and large magnification TEM images of ultrathin sections of the nanocomposite films, and c) FIB-SEM image of the same material highlighting the remarkable homogeneity of the clay network at a very large scale. Reproduced from ref.<sup>19</sup> with permission from Elsevier.

The effect of surfactant on the mechanical properties of NBR latex/LDH composites obtained by coagulation, was studied by Braga et al.<sup>21</sup> It was shown that the addition of a surfactant

significantly improved LDH dispersion in the NBR matrix as confirmed indirectly by a lower Payne effect. The Payne effect is a particular feature of filled rubbers, characterized by the pronounced decrease of the storage modulus with increasing strain amplitude reflecting agglomeration of the filler particles due to filler-filler interactions. The nanocomposites obtained in the presence of surfactant showed a substantially lower variation of the shear modulus with the shear strain ( $\Delta G^* = 5.59$  KPa) than the system without surfactant ( $\Delta G^* = 14.29$  KPa) suggesting a better dispersion of the LDH platelets.

Bao et al.<sup>30</sup> reported the mechanical properties of PVDC/LDH-DS composites synthesized by suspension polymerization for increasing LDH contents. The young's modulus, the tensile strength and the Charpy notched impact strength were all greater than those of pristine PVC and PVC/LDH-DS composites obtained by melt-blending, and all leveled off with increasing LDH content (Figure 13).

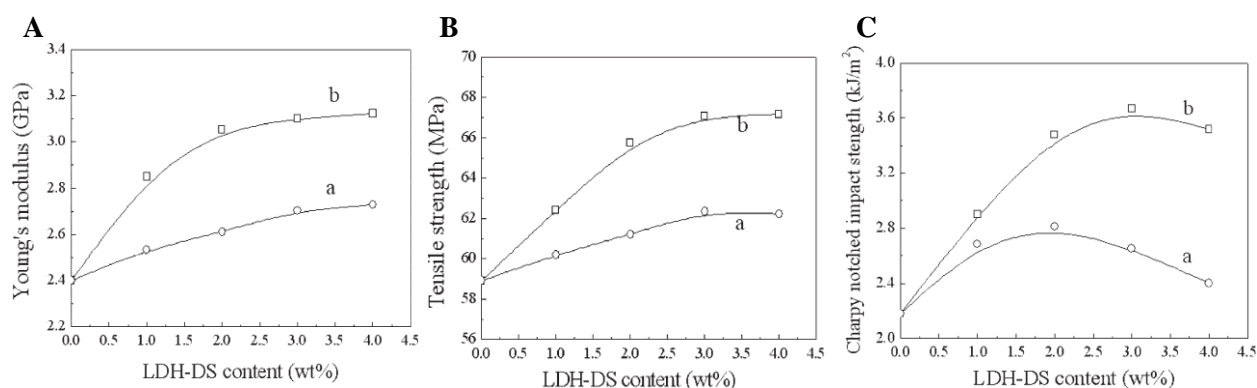


**Figure 13.** Influence of LDH-DS weight fraction on: A) Young's modulus, B) tensile strength and C) Charpy notched impact strength of PVC/LDH-DS composites. a) melt-blending and b) *in situ* suspension polymerization. Reproduced from ref.<sup>30</sup>. Copyright 2016 Wiley Periodicals, Inc.

The increased mechanical performances were attributed in this case to a better clay dispersion in the polymer matrix and stronger clay/polymer interfacial interactions.

### 3.1.2 Flame retardancy

Zhao et al.<sup>22a</sup> investigated the flame retardancy properties of P(BA-*co*-VAc) membranes containing ammonium polyphosphate (APP) – a halogen-free flame retardant - and organically-modified LDH platelets (O-LDH). The films were obtained by casting an O-LDH/APP/P(BA-*co*-VAc) latex suspension obtained by *in situ* emulsion polymerization of BA and VAc in the presence of APP and clay, and evaporating the water at room temperature for 3 days followed by vacuum drying at 50 °C. Thermal gravimetric analysis showed that the composite sample displayed a higher solid residue (curve e in Figure 14A) than calculated from the clay and APP contents (curve b, Figure 14A).

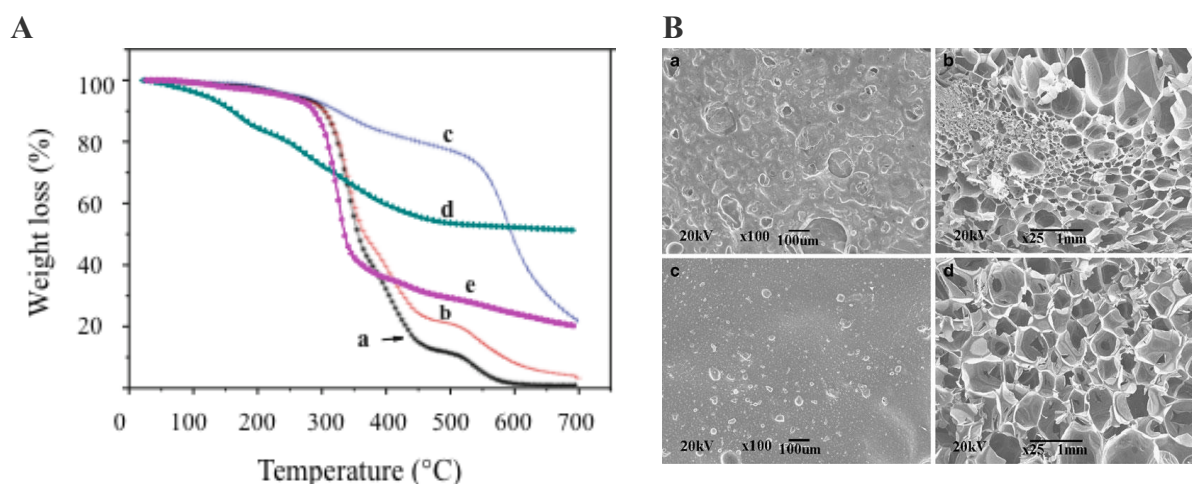


**Figure 14.** A) TGA curves of: a) P(BA-*co*-VAc), b) O-LDH/APP/P(BA-*co*-VAc) calculated, c) APP, d) O-LDH and e) O-LDH/APP/P(BA-*co*-VAc) experimental. B) SEM images of the char samples obtained for a, b) APP/P(BA-*co*-VAc) and c, d) O-LDH/APP/P(BA-*co*-VAc) (a, c : outer surfaces and b, d) inner surfaces. Reproduced from ref.<sup>22a</sup> Copyright 2011 Springer.

The thermal behavior was thus not just the sum of the thermal degradations of the individual components but an additional stabilization mechanism was at play. Indeed, FTIR and XPS analysis showed the formation, during pyrolysis and combustion, of polyphosphoric and aromatic structures. The authors argued that O-LDH could catalyze the formation of a three dimensional network by reaction of APP degradation products with the polymer chains resulting in crosslinking and compact char formation. SEM further confirmed the homogeneous and dense structure of the inner and outer char (Figure 15C). The intumescent char residues formed a protective layer on the outer surface of the composite material preventing further combustion at high temperatures.

### 3.2 LDH-based macroporous structures

Numerous potential applications of macroporous LDH materials can be considered including mainly chemical applications that rely on the enhanced porosity, high surface area and rapid molecular diffusion within the interconnected nanostructured materials. In the following, the specific properties and applications of hollow nanostructured and macroporous LDHs obtained using latex templating approaches are summarized, focusing on applications such as adsorption, sensing, catalysis/photocatalysis and the development of electrochemical devices.

#### 3.2.1 Adsorption and extraction

As porous hosts, LDH materials prepared using PS templating approaches are obvious candidates for adsorption and extraction processes. Chloride entrapment was investigated using core/shell PS/MgAl-NO<sub>3</sub> evidencing that equilibrium was reached after 4h. The highest uptake capacity equal to 510.85 mg g<sup>-1</sup> was recorded at pH 8 corresponding to a removal

percentage of 51.55%. Unfortunately, the role of the PS core was not elucidated in this study and the comparison with the hollow LDH spheres resulting from the PS core removal, not provided. Enhanced loading of adsorbates on nanostructured LDHs has also been demonstrated for anionic dye molecules, such as orange II.<sup>55c</sup> 3-DOM MgAl-CO<sub>3</sub> LDH displayed very high adsorption capacities toward orange II, especially the calcined LDH materials (4.34 mmol g<sup>-1</sup>) compared to the standard MgAl-CO<sub>3</sub> LDH phase (0.504 mmol g<sup>-1</sup>). Such difference was attributed to a better accessibility to the LDH layer surface. While MgAl-CO<sub>3</sub> phases mainly displayed a surface exchange chemisorption process, the calcined LDH phases gave rise to the highest concentrations of adsorbed O-II due to a partial intercalation of O-II molecules through the calcination/reconstruction phenomenon. The interest of 3-DOM LDH materials was also shown for solid-phase microextraction of phenolic and polycyclic aromatic hydrocarbon compounds.<sup>64</sup> Due to their pore structure, large surface area and homogenous macroporous morphology, enhanced adsorption capacity was obtained and compared favorably to commercial materials such as polydimethylsiloxane, allowing successful pre-concentration of phenolic compounds in water samples.<sup>55c, 64</sup>

### 3.2.2 Catalysis and photocatalysis

The introduction of porosity increases surface area and ensures a good mass transport through interconnected pores and from large interfaces. These properties contribute to the high catalytic activity of LDH-based materials. LDHs have been reported as heterogeneous base catalysts for the transesterification of triglycerides;<sup>65</sup> however their efficiency is hampered by restricted diffusion of bulky triglycerides within the crystallites.<sup>66</sup> Woodford et al. studied the production of triacylglycerides (C<sub>3</sub>H<sub>5</sub>(OOR)<sub>3</sub> R= C<sub>4</sub>, C<sub>8</sub> and C<sub>12</sub>) or unsaturated glyceryl diesel.<sup>52</sup> They demonstrated that the macropores conferred significant benefits for

transesterification especially the triglycerides of long chain, due to improved diffusion and accessibility to the active sites. For instance, a ten-fold rate enhancement was observed for triolein in using macroporous LDH compared to conventional LDH with improved conversion and without loss of fatty acid methyl esters selectivity. In addition, macroporous LDHs with well-defined porosity have been used as a bidimensional support to intercalate or immobilize homogenous catalytic species. Anionic iron (III) porphyrins of first and second generation were immobilized on macroporous LDH phases using both the calcination reconstruction phenomenon and the anionic exchange and investigated as catalysts for cyclooctene, cyclohexane and heptane oxidation.<sup>55a</sup> The results obtained showed that the efficiency and selectivity of the metalloporphyrins immobilized on/in macroporous LDH changed. A good selectivity for the alcohol product was systematically observed for the macroporous heterogenous phases. Decatungstate  $W_{10}O_{32}^{4-}$  was also efficiently intercalated into 3-DOM MgAl-LDHs to produce heterogeneous photocatalysts. The photocatalytic activity of  $W_{10}O_{32}^{4-}$  immobilized on both macroporous and conventional LDH was tested with two pollutants: the 2, 4 dimethylphenol and the 2-(1-naphthyl) acetamide. The presence of macropores drastically increased the accessibility of light and the efficiency of the photodegradation. For instance, 60% of 2-(1-naphthyl) acetamide were photodegraded ( $\lambda=365$  nm) after 17h at pH 6.6 for an optimal concentration of photocatalyst of  $60 \text{ mg L}^{-1}$ . Complete mineralization of the pesticide was observed and the photocatalyst could be reused over four cycles without loss of activity.

### 3.2.3 Electrochemical and magnetic properties

Electrochemical devices made of 3DOM LDH capitalize on the relatively large and accessible surfaces in the modified electrodes. Usually, the electrodes are based on thin LDH films electrodeposited on a conductive support.<sup>57-58</sup> The presence of redox metal cations such as Ni or Co into the LDH layers confers electrochemical properties to LDH membranes. Compared to a bare flat LDH electrode,<sup>67</sup> a 3-DOM NiAl LDH-modified electrode was shown to exhibit greater permeability and was further used to develop an amperometric electrochemical biosensing device for the detection of glucose.<sup>57a</sup> The nanostructured electrode was used to immobilized glucose oxidase. An increase of sensitivity from 13 to 18 mA M<sup>-1</sup> cm<sup>-2</sup> was measured for the nanostructured LDH film compared to the compact film, which was ascribed to the higher porosity facilitating glucose diffusion. Electrosynthesized 3DOM LDH electrode was also used as an electrochromic coating.<sup>57b</sup> Transmittance changes were followed by *in situ* measurements of the UV-vis spectra during potential cycling showing a change in relative transmittance four times larger than the change observed for the compact film (Figure 15). It was underlined that the reversibility of the color change was greatly improved by heating the films to convert the LDH phase to the corresponding mixed oxides.

Magnetic properties of spinel nanostructured microspheres obtained from CoFe<sup>II</sup>Fe<sup>III</sup>- and Ni<sub>0.5</sub>Co<sub>0.5</sub>Fe<sup>II</sup>Fe<sup>III</sup>- LDH microsphere precursors were investigated. In using an appropriate M<sup>II</sup>/ (Fe<sup>II</sup>+Fe<sup>III</sup>) ratio in the LDH precursor phase, pure spinel M<sup>II</sup>Fe<sub>2</sub>O<sub>4</sub> was synthesized by simple calcination at 900 °C in air. Thanks to the great versatility of composition in the LDH layer, the magnetic properties of the resulting spinels could be tuned over a large range.<sup>68</sup> CoFe<sup>II</sup>Fe<sup>III</sup>- and Ni<sub>0.5</sub>Co<sub>0.5</sub>Fe<sup>II</sup>Fe<sup>III</sup>-LDH raspberry-like hollow spheres retained their morphology upon heating, leading to Ni<sub>0.5</sub>Co<sub>0.5</sub>Fe<sub>2</sub>O<sub>4</sub> microspheres displaying unmodified magnetic properties compared to spinels obtained from conventional LDH powder. These could be of interest in applications as drug carriers or catalysts.<sup>51</sup> Similarly, CoFe<sub>2</sub>O<sub>4</sub>

microspheres prepared from LDH microsphere precursors obtained by combining spray drying and PS templating displayed a saturation magnetization of  $52.8 \text{ emu g}^{-1}$  and a coercive force of 205 Oe which is comparable to the powdered LDH precursors.

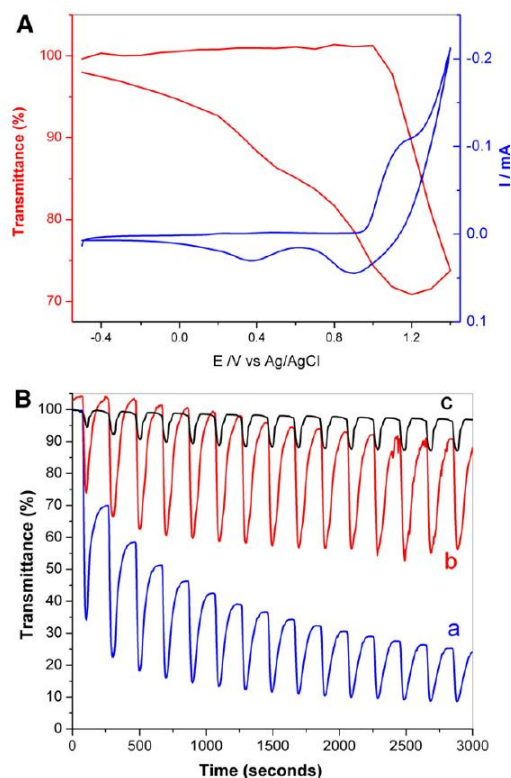


**Figure 15.** A. Transmittance (red) and current (blue) versus potential curves obtained for an inverted opal structure Ni-Al-LDH coating in presence of  $0.1 \text{ mM } [\text{Fe}(\text{CN})_6]^{4-}$  ( $20 \text{ mV s}^{-1}$  in  $0.1 \text{ M}$  borate buffer at pH 8). B. Transmittance versus time of an inverted opal Ni-Al-LDH film in the absence (a) and presence (b) of  $0.1 \text{ mM } [\text{Fe}(\text{CN})_6]^{4-}$ . (c) Transmittance versus time for a non inverted film in presence of  $[\text{Fe}(\text{CN})_6]^{4-}$  (first 15 scans at  $20 \text{ mV s}^{-1}$  between  $-0.5$  and  $1.4 \text{ V}$  vs. Ag/AgCl in a  $0.1 \text{ M}$  borate buffer at pH 8). Reproduced from ref. <sup>57b</sup> with permission from Elsevier.

#### 4- Concluding remarks and general trends

Over the last decade, the use of latex technology has become a powerful tool for the production of LDH-based composite materials and macroporous structures. As illustrated in this chapter, several approaches have been described including the assembly of preformed LDH and latex particles, *in-situ* emulsion or suspension polymerization in the presence of LDH particles and the use of polymer latexes as sacrificial templates. Even if their synthesis is often challenging, the large panel of LDH synthetic pathways using soft chemistry conditions has recently allowed the successful preparation of stable LDH colloidal suspensions and well-defined LDH/polymer composite particles. The control of synthetic process and the increased level of understanding have enabled the design of original morphologies which were until recently difficult to achieve. These include LDH-armoured latex particles, polymer-encapsulated LDHs, LDH inverse opals, and LDH hollow spheres. Waterborne LDH/polymer nanocomposites obtained by latex technology display great promise for the development of coatings with improved mechanical and flame-retardant properties. In addition, nanostructured LDH materials prepared by the latex templating approach possessed real advantages for various applications such as adsorption for environmental purposes and photo/electro-catalysis. On the basis of the recent progress observed in this field, we strongly believe that more is to come for the development of LDH/polymer nanocomposite latexes. Some of the major possibilities may be in the preparation of nanostructured multicomponent systems by employing new functional hybrid LDH particles and introducing additional particles to open up new applications for LDH-based materials.

## REFERENCES

1. (a) Fellingine, F.; Rosato, C.; Scatto, M.; Tinti, A.; Scopece, P.; Nacucchi, M., Active Polymer Nanocomposites: Application in Thermoplastic Polymers and in Polymer Foams. *IEEE T. Nanotechnol.* **2016**, *15*, 896-903; (b) Kumar, S. K.; Benicewicz, B. C.; Vaia, R. A.; Winey, K. I., 50th Anniversary Perspective: Are Polymer Nanocomposites Practical for Applications? *Macromolecules* **2017**, *50*, 714-731.
2. (a) Galimberti, M.; Cipolletti, V. R.; Coombs, M., Chapter 4.4 - Applications of Clay–Polymer Nanocomposites. In *Developments in Clay Science*, Faïza, B.; Gerhard, L., Eds. Elsevier: 2013; Vol. Volume 5, pp 539-586; (b) Ray, S. S., Recent Trends and Future Outlooks in the Field of Clay-Containing Polymer Nanocomposites. *Macromol. Chem. Phys.* **2014**, *215*, 1162-1179.
3. Lambert, J. F.; Bergaya, F., Chapter 13.1 - Smectite–Polymer Nanocomposites. In *Developments in Clay Science*, Faïza, B.; Gerhard, L., Eds. Elsevier: 2013; Vol. Volume 5, pp 679-706.
4. (a) Leroux, F.; Besse, J.-P., Polymer Interleaved Layered Double Hydroxide: A New Emerging Class of Nanocomposites. *Chem. Mater.* **2001**, *13*, 3507-3515; (b) Costa, F. R.; Saphiannikova, M.; Wagenknecht, U.; Heinrich, G., Layered Double Hydroxide Based Polymer Nanocomposites. *Adv. Polym. Sci.* **2008**, *210*, 101-168; (c) Matusinovic, Z.; Wilkie, C. A., Fire retardancy and morphology of layered double hydroxide nanocomposites: a review *J. Mater. Chem.* **2012**, *22*, 18701-18704; (d) Rives, V. L., Francisco M.; Herrero, Mar Effect of preparation procedures on the properties of LDH/organo nanocomposites In *Nanocomposite*, Wang, X., Ed. 2013; pp 169-202; (e) Gao, Y.; Wu, J.; Wang, Q.; Wilkie, C. A.; O'Hare, D., Flame retardant polymer/layered double hydroxide nanocomposites *J. Mater. Chem. A* **2014**, *2*, 10996-11016; (f) Basu, D.; Das, A.; Stockelhuber, K. W.; Wagenknecht, U.; Heinrich, G., Advances in layered double hydroxide (LDH)-based elastomer composites. *Prog. Polym. Sci.* **2014**, *39*, 594-626; (g) Kalali, E. N.; Wang, X.; Wang, D.-Y.,

Functionalized layered double hydroxide-based epoxy nanocomposites with improved flame retardancy and mechanical properties. *J. Mater. Chem. A* **2015**, *3*, 6819-6826.

5. (a) Rives, V., *Layered Double Hydroxides: Present and Future*. Nova Science: New York, 2001; p 439; (b) Duan, X.; Evans, D. G.; Editors, *Structure and bonding : Layered Double Hydroxides*. Springer: Berlin/Heidelberg, 2006; Vol. 119; (c) Costantino, U.; Leroux, F.; Nocchetti, M.; Mousty, C., LDH in physical, chemical, bio-chemical and life science. In *Handbook of Clay Science*, Faiza Bergaya, G. L. E., Ed. Elsevier Amsterdam, The Netherlands: 2013; Vol. 5, pp 765-791; (d) Forano, C.; Costantino, U.; Prevot, V.; Taviot Gueho, C., Layered Double Hydroxides. In *Handbook of Clay Science* Faiza Bergaya, G. L., Ed. Elsevier: Amsterdam, 2013; Vol. 5, pp 745-783.

6. (a) Xu, Z. P.; Stevenson, G.; Lu, C.-Q.; Lu, G. Q., Dispersion and Size Control of Layered Double Hydroxide Nanoparticles in Aqueous Solutions. *J. Phys. Chem. B* **2006**, *110*, 16923-16929; (b) Xu, Z. P.; Stevenson, G. S.; Lu, C.-Q.; Lu, G. Q.; Bartlett, P. F.; Gray, P. P., Stable Suspension of Layered Double Hydroxide Nanoparticles in Aqueous Solution. *J. Am. Chem. Soc.* **2006**, *128*, 36-37; (c) Gunawan, P.; Xu, R., Direct Assembly of Anisotropic Layered Double Hydroxide (LDH) Nanocrystals on Spherical Template for Fabrication of Drug-LDH Hollow Nanospheres. *Chem. Mater.* **2009**, *21*, 781-783.

7. Okamoto, K.; Iyi, N.; Sasaki, T., Factors affecting the crystal size of the MgAl-LDH (layered double hydroxide) prepared by using ammonia-releasing reagents. *Appl. Clay Sci.* **2007**, *37*, 23-31.

8. Wang, Q.; O'Hare, D., Recent Advances in the Synthesis and Application of Layered Double Hydroxide (LDH) Nanosheets. *Chem. Rev.* **2012**, *112*, 4124-4155.

9. Qiu, L.; Qu, B., Chapter 2 Polymer-Layered Double Hydroxide Nanocomposites by Emulsion and Suspension Polymerization. In *Polymer Nanocomposites by Emulsion and Suspension Polymerization*, The Royal Society of Chemistry: 2011; pp 32-63.

10. Bourgeat-Lami, E.; Lansalot, M., Organic/Inorganic Composite Latexes: The Marriage of Emulsion Polymerization and Inorganic Chemistry. *Adv. Polym. Sci.* **2010**, *233*, 53-123.
11. Decher, G., Fuzzy Nanoassemblies: Toward Layered Polymeric Multicomposites. *Science* **1997**, *277*, 1232.
12. (a) Li, L.; Ma, R.; Ebina, Y.; Iyi, N.; Sasaki, T., Positively Charged Nanosheets Derived via Total Delamination of Layered Double Hydroxides. *Chem. Mater.* **2005**, *17*, 4386-4391; (b) Liu, Z.; Ma, R.; Osada, M.; Iyi, N.; Ebina, Y.; Takada, K.; Sasaki, T., Synthesis, Anion Exchange, and Delamination of Co–Al Layered Double Hydroxide: Assembly of the Exfoliated Nanosheet/Polyanion Composite Films and Magneto-Optical Studies. *J. Am. Chem. Soc.* **2006**, *128*, 4872-4880; (c) Han, J. B.; Lu, J.; Wei, M.; Wang, Z. L.; Duan, X., Heterogeneous ultrathin films fabricated by alternate assembly of exfoliated layered double hydroxides and polyanion. *Chem. Commun.* **2008**, 5188-5190; (d) Guo, X.; Zhang, F.; Evans, D. G.; Duan, X., Layered double hydroxide films: synthesis, properties and applications. *Chem. Commun.* **2010**, *46*, 5197-5210.
13. Li, L.; Ma, R.; Iyi, N.; Ebina, Y.; Takada, K.; Sasaki, T., Hollow nanoshell of layered double hydroxide. *Chem. Commun.* **2006**, 3125-3127.
14. Bujdosó, T.; Hornok, V.; Dékány, I., Thin films of layered double hydroxide and silver-doped polystyrene particles. *Appl. Clay Sci.* **2011**, *51*, 241-249.
15. Regev, O.; ElKati, P. N. B.; Loos, J.; Koning, C. E., Preparation of Conductive Nanotube–Polymer Composites Using Latex Technology. *Adv. Mater.* **2004**, *16*, 248-251.
16. Noël, A.; Faucheu, J.; Chenal, J.-M.; Viricelle, J.-P.; Bourgeat-Lami, E., Electrical and mechanical percolation in graphene-latex nanocomposites. *Polymer* **2014**, *55*, 5140-5145.

17. Prasertsri, S.; Lagarde, F.; Rattanasom, N.; Sirisinha, C.; Daniel, P., Raman spectroscopy and thermal analysis of gum and silica-filled NR/SBR blends prepared from latex system. *Polym. Test.* **2013**, *32*, 852-861.
18. Bourgeat-Lami, E.; Faucheu, J.; Noël, A., Latex routes to graphene-based nanocomposites. *Polym. Chem.* **2015**, *6*, 5323-5357.
19. Veschambres, C.; Halma, M.; Bourgeat-Lami, E.; Chazeau, L.; Dalmas, F.; Prevot, V., Layered double hydroxides: Efficient fillers for waterborne nanocomposite films. *Appl. Clay Sci.* **2016**, *130*, 55-61.
20. Pavlovic, M.; Rouster, P.; Bourgeat-Lami, E.; Prevot, V.; Szilagy, I., Design of latex-layered double hydroxide composites by tuning the aggregation in suspensions. *Soft Matter* **2017**, *13*, 842-851.
21. Braga, F. C. F.; Furtado, C. R. G.; Oliveira, M. G., Influence of the Surfactant on the Hydrotalcite Dispersion in NBR/LDH Composites Produced by Coagulation. *Macromol. Symp.* **2014**, *343*, 70-77.
22. (a) Zhao, C.; Peng, G.; Liu, B.; Jiang, Z., Synergistic effect of organically modified layered double hydroxide on thermal and flame-retardant properties of poly(butyl acrylate–vinyl acetate). *J. Polym. Res.* **2011**, *18*, 1971-1981; (b) Usuki, A.; Kawasumi, M.; Kojima, Y.; Okada, A.; Kurauchi, T.; Kamigaito, O., Swelling behavior of montmorillonite cation exchanged for  $\omega$ -amino acids by  $\epsilon$ -caprolactam. *J. Mater. Res.* **1993**, *8*, 1174-1178; (c) Usuki, A.; Kojima, Y.; Kawasumi, M.; Okada, A.; Fukushima, Y.; Kurauchi, T.; Kamigaito, O., Synthesis of nylon 6-clay hybrid. *J. Mater. Res.* **1993**, *8*, 1179-1184.
23. Chern, C. S., Emulsion polymerization mechanisms and kinetics. *Prog. Polym. Sci.* **2006**, *31*, 443-486.
24. Bourgeat-Lami, E.; Sheibat-Othman, N.; Dos Santos, A. M., Chapter 13 Polymer-Clay Nanocomposite Particles and Soap-free Latexes Stabilized by Clay Platelets: State of the Art

and Recent Advances. In *Polymer Nanocomposites by Emulsion and Suspension Polymerization*, The Royal Society of Chemistry: 2011; pp 269-311.

25. Chen, W.; Feng, L.; Qu, B., In situ synthesis of poly(methyl methacrylate)/MgAl layered double hydroxide nanocomposite with high transparency and enhanced thermal properties. *Solid State Commun.* **2004**, *130*, 259-263.

26. Ding, P.; Qu, B., Synthesis and characterization of exfoliated polystyrene/ZnAl layered double hydroxide nanocomposite via emulsion polymerization. *J. Colloid Interface Sci.* **2005**, *291*, 13-18.

27. Ding, P.; Qu, B., Synthesis and characterization of polystyrene/layered double-hydroxide nanocomposites via in situ emulsion and suspension polymerization. *J. Appl. Polym. Sci.* **2006**, *101*, 3758-3766.

28. Qiu, L.; Qu, B., Preparation and characterization of surfactant-free polystyrene/layered double hydroxide exfoliated nanocomposite via soap-free emulsion polymerization. *J. Colloid Interface Sci.* **2006**, *301*, 347-351.

29. Kovanda, F.; Jindová, E.; Lang, K.; Kubát, P.; Sedláková, Z., Preparation of layered double hydroxides intercalated with organic anions and their application in LDH/poly(butyl methacrylate) nanocomposites. *Appl. Clay Sci.* **2010**, *48*, 260-270.

30. Bao, Y.-Z.; Huang, Z.-M.; Weng, Z.-X., Preparation and characterization of poly(vinyl chloride)/layered double hydroxides nanocomposite via in situ suspension polymerization. *J. Appl. Polym. Sci.* **2006**, *102*, 1471-1477.

31. Pyun, J.; Matyjaszewski, K., Synthesis of Nanocomposite Organic/Inorganic Hybrid Materials Using Controlled/"Living" Radical Polymerization. *Chem. Mater.* **2001**, *13*, 3436-3448.

32. Barbey, R.; Lavanant, L.; Paripovic, D.; Schüwer, N.; Sugnaux, C.; Tugulu, S.; Klok, H.-A., Polymer Brushes via Surface-Initiated Controlled Radical Polymerization: Synthesis, Characterization, Properties, and Applications. *Chem. Rev.* **2009**, *109*, 5437-5527.
33. Roghani-Mamaqani, H.; Haddadi-Asl, V.; Salami-Kalajahi, M., In Situ Controlled Radical Polymerization: A Review on Synthesis of Well-defined Nanocomposites. *Polymer Reviews* **2012**, *52*, 142-188.
34. Francis, R.; Joy, N.; Aparna, E. P.; Vijayan, R., Polymer Grafted Inorganic Nanoparticles, Preparation, Properties, and Applications: A Review. *Polymer Reviews* **2014**, *54*, 268-347.
35. Hui, C. M.; Pietrasik, J.; Schmitt, M.; Mahoney, C.; Choi, J.; Bockstaller, M. R.; Matyjaszewski, K., Surface-Initiated Polymerization as an Enabling Tool for Multifunctional (Nano-)Engineered Hybrid Materials. *Chem. Mater.* **2014**, *26*, 745-762.
36. Konn, C.; Morel, F.; Beyou, E.; Chaumont, P.; Bourgeat-Lami, E., Nitroxide-mediated polymerization of styrene initiated from the surface of laponite clay platelets. *Macromolecules* **2007**, *40*, 7464-7472.
37. Qiu, L. Z.; Chen, W.; Qu, B. J., Exfoliation of layered double hydroxide in polystyrene by in-situ atom transfer radical polymerization using initiator-modified precursor. *Colloid Polym. Sci.* **2005**, *283*, 1241-1245.
38. Hu, H.; Xiu, K. M.; Xu, S. L.; Yang, W. T.; Xu, F. J., Functionalized Layered Double Hydroxide Nanoparticles Conjugated with Disulfide-Linked Polycation Brushes for Advanced Gene Delivery. *Bioconjug. Chem.* **2013**, *24*, 968-978.
39. Ding, P.; Zhang, M.; Gai, J.; Qu, B. J., Homogeneous dispersion and enhanced thermal properties of polystyrene-layered double hydroxide nanocomposites prepared by in situ reversible addition-fragmentation chain transfer (RAFT) polymerization. *J. Mater. Chem.* **2007**, *17*, 1117-1122.

40. Reddy, M. V.; Lien, N. T. K.; Reddy, G. C. S.; Lim, K. T.; Jeong, Y. T., Polymer grafted layered double hydroxides (LDHs-g-POEGMA): a highly efficient reusable solid catalyst for the synthesis of chromene incorporated dihydroquinoline derivatives under solvent-free conditions. *Green Chem.* **2016**, *18*, 4228-4239.
41. Zetterlund, P. B.; Thickett, S. C.; Perrier, S.; Bourgeat-Lami, E.; Lansalot, M., Controlled/Living Radical Polymerization in Dispersed Systems: An Update. *Chem. Rev.* **2015**, *115*, 9745-800.
42. Cenacchi-Pereira, A.; Grant, E.; D'Agosto, F.; Lansalot, M.; Bourgeat-Lami, E., Encapsulation with the Use of Controlled Radical Polymerization. In *Encyclopedia of Polymeric Nanomaterials*, Kobayashi, S.; Müllen, K., Eds. Springer Berlin Heidelberg: 2015; pp 718-729.
43. Bourgeat-Lami, E.; D'Agosto, F.; Lansalot, M., Synthesis of Nanocapsules and Polymer/Inorganic Nanoparticles Through Controlled Radical Polymerization At and Near Interfaces in Heterogeneous Media. In *Controlled Radical Polymerization at and from Solid Surfaces*, Vana, P., Ed. Springer International Publishing: 2016; Vol. 270, pp 123-161.
44. Qiao, X. G.; Dugas, P. Y.; Charleux, B.; Lansalot, M.; Bourgeat-Lami, E., Synthesis of Multipod-like Silica/Polymer Latex Particles via Nitroxide-Mediated Polymerization-Induced Self-Assembly of Amphiphilic Block Copolymers. *Macromolecules* **2015**, *48*, 545-556.
45. Loiko, O. P.; Spoelstra, A. B.; van Herk, A. M.; Meuldijk, J.; Heuts, J. P. A., An ATRP-based approach towards water-borne anisotropic polymer-Gibbsite nanocomposites. *Polym. Chem.* **2016**, *7*, 3383-3391.
46. Cenacchi, A.; Pearson, S.; Kostadinova, D.; Leroux, F.; D'Agosto, F.; Lansalot, M.; Bourgeat-Lami, E.; Prevot, V., Nanocomposite latexes containing layered double hydroxides

via RAFT-assisted encapsulating emulsion polymerization. *Polym. Chem.* **2017**, *8*, 1233-1243.

47. Ma, Y.; Qi, L., Solution-phase synthesis of inorganic hollow structures by templating strategies. *J. Colloid Interface Sci.* **2009**, *335*, 1-10.

48. (a) Stein, A.; Wilson, B. E.; Rudisill, S. G., Design and functionality of colloidal-crystal-templated materials-chemical applications of inverse opals. *Chem. Soc. Rev.* **2013**, *42*, 2763-2803; (b) Petkovich, N. D.; Stein, A., Controlling macro- and mesostructures with hierarchical porosity through combined hard and soft templating. *Chem. Soc. Rev.* **2013**, *42*, 3721-3739.

49. Du, Y.; Hu, G.; O'Hare, D., Nucleation and growth of oriented layered hydroxides on polymer resin beads. *J. Mater. Chem.* **2009**, *19*, 1160-1165.

50. Kartsonakis, I. A.; Karaxi, E. K.; Charitidis, C. A., Evaluation of polymer composites based on core/shell polystyrene/Mg-Al-NO<sub>3</sub> layered double hydroxides for chloride entrapment. *Plastics, Rubber and Composites* **2016**, *45*, 50-57.

51. Xu, S.; Yang, Y.; Xu, T.; Kuang, Y.; Dong, M.; Zhang, F.; Besenbacher, F.; Evans, D. G., Engineered morphologies of layered double hydroxide nanoarchitected shell microspheres and their calcined products. *Chem. Eng. Sci.* **2011**, *66*, 2157-2163.

52. Woodford, J. J.; Dacquin, J.-P.; Wilson, K.; Lee, A. F., Better by design: nanoengineered macroporous hydrotalcites for enhanced catalytic biodiesel production. *Energy Environ. Sci.* **2012**, *5*, 6145-6150.

53. Zhao, Y.; Li, F.; Zhang, R.; Evans, D. G.; Duan, X., Preparation of Layered Double-Hydroxide Nanomaterials with a Uniform Crystallite Size Using a New Method Involving Separate Nucleation and Aging Steps. *Chem. Mater.* **2002**, *14*, 4286-4291.

54. Zhang, F.; Xie, Y.; Xu, S.; Zhao, X.; Lei, X., Facile fabrication and magnetic properties of macroporous spinel microspheres from layered double hydroxide microsphere precursor. *Chem. Lett.* **2010**, *39*, 588-590.
55. (a) Halma, M.; Castro, K. A. D. d. F.; Prevot, V.; Forano, C.; Wypych, F.; Nakagaki, S., Immobilization of anionic iron(III) porphyrins into ordered macroporous layered double hydroxides and investigation of catalytic activity in oxidation reactions. *J. Mol. Catal. A: Chem.* **2009**, *310*, 42-50; (b) Geraud, E.; Rafqah, S.; Sarakha, M.; Forano, C.; Prevot, V.; Leroux, F., Three Dimensionally Ordered Macroporous Layered Double Hydroxides: Preparation by Templated Impregnation/Coprecipitation and Pattern Stability upon Calcination. *Chem. Mater.* **2008**, *20*, 1116-1125; (c) Geraud, E.; Bouhent, M.; Derriche, Z.; Leroux, F.; Prevot, V.; Forano, C., Texture effect of layered double hydroxides on chemisorption of Orange II. *J. Phys. Chem. Solids* **2007**, *68*, 818-823; (d) Geraud, E.; Prevot, V.; Leroux, F., Synthesis and characterization of macroporous MgAl LDH using polystyrene spheres as template. *J. Phys. Chem. Solids* **2006**, *67*, 903-908; (e) Geraud, E.; Prevot, V.; Ghanbaja, J.; Leroux, F., Macroscopically Ordered Hydrotalcite-Type Materials Using Self-Assembled Colloidal Crystal Template. *Chem. Mater.* **2006**, *18*, 238-240.
56. Prevot, V.; Geraud, E.; Stimpfling, T.; Ghanbaja, J.; Leroux, F., Hierarchically structured carbon replica of hybrid layered double hydroxide. *New J. Chem.* **2011**, *35*, 169-177.
57. (a) Prevot, V.; Forano, C.; Khenifi, A.; Ballarin, B.; Scavetta, E.; Mousty, C., A templated electrosynthesis of macroporous NiAl layered double hydroxides thin films. *Chem. Commun.* **2011**, *47*, 1761-1763; (b) Martin, J.; Jack, M.; Hakimian, A.; Vaillancourt, N.; Villemure, G., Electrodeposition of Ni-Al layered double hydroxide thin films having an inversed opal structure: Application as electrochromic coatings. *J. Electroanal. Chem.* **2016**, *780*, 217-224.

58. Scavetta, E.; Mignani, A.; Prandstraller, D.; Tonelli, D., Electrosynthesis of Thin Films of Ni, Al Hydrotalcite Like Compounds. *Chem. Mater.* **2007**, *19*, 4523-4529.
59. Tokudome, Y.; Morimoto, T.; Tarutani, N.; Vaz, P. D.; Nunes, C. D.; Prevot, V.; Stenning, G. B. G.; Takahashi, M., Layered Double Hydroxide Nanoclusters: Aqueous, Concentrated, Stable, and Catalytically Active Colloids toward Green Chemistry. *ACS Nano* **2016**, *10*, 5550-5559.
60. Chabert, E.; Bornert, M.; Bourgeat-Lami, E.; Cavaille, J.; Dendievel, R.; Gauthier, C.; Putaux, U.; Zaoui, A., Filler-filler interactions and viscoelastic behavior of polymer nanocomposites. *Materials Science and Engineering a-Structural Materials Properties Microstructure and Processing* **2004**, *381*, 320-330.
61. Negrete-Herrera, N.; Putaux, J.-L.; David, L.; De Haas, F.; Bourgeat-Lami, E., Polymer/Laponite composite latexes: Particle morphology, film microstructure, and properties. *Macromolecular Rapid Communications* **2007**, *28*, 1567-1573.
62. Ruggerone, R.; Plummer, C. J. G.; Herrera, N. N.; Bourgeat-Lami, E.; Manson, J.-A. E., Highly filled polystyrene-laponite nanocomposites prepared by emulsion polymerization. *European Polymer Journal* **2009**, *45*, 621-629.
63. Ruggerone, R.; Plummer, C. J. G.; Herrera, N. N.; Bourgeat-Lami, E.; Manson, J.-A. E.; Kny, E., Mechanical properties of highly filled latex-based polystyrene/laponite nanocomposites. *Solid State Phenomena* **2009**, *151*, 30-34.
64. Abolghasemi, M. M.; Yousefi, V., Three dimensionally honeycomb layered double hydroxides framework as a novel fiber coating for headspace solid-phase microextraction of phenolic compounds. *J. Chromatogr. A* **2014**, *1345*, 9-16.
65. He, S.; An, Z.; Wei, M.; Evans, D. G.; Duan, X., Layered double hydroxide-based catalysts: nanostructure design and catalytic performance. *Chem. Commun.* **2013**, *49*, 5912-5920.

66. (a) Cantrell, D. G.; Gillie, L. J.; Lee, A. F.; Wilson, K., Structure-reactivity correlations in MgAl hydrotalcite catalysts for biodiesel synthesis. *Appl. Catal. A*. **2005**, *287*, 183-190; (b) Xi, Y.; Davis, R. J., Influence of water on the activity and stability of activated MgAl hydrotalcites for the transesterification of tributyrin with methanol. *J. Catal.* **2008**, *254*, 190-197; (c) Kim, M. J.; Park, S. M.; Chang, D. R.; Seo, G., Transesterification of triacetin, tributyrin, and soybean oil with methanol over hydrotalcites with different water contents. *Fuel Process. Technol.* **2010**, *91*, 618-624.
67. (a) Mousty, C., Sensors and biosensors based on clay-modified electrodes - new trends. *Appl. Clay Sci.* **2004**, *27*, 159-177; (b) Shao, M.; Zhang, R.; Li, Z.; Wei, M.; Evans, D. G.; Duan, X., Layered double hydroxides toward electrochemical energy storage and conversion: design, synthesis and applications. *Chem. Commun.* **2015**, *51*, 15880-15893.
68. Abellan, G.; Marti-Gastaldo, C.; Ribera, A.; Coronado, E., Hybrid Materials Based on Magnetic Layered Double Hydroxides: A Molecular Perspective. *Acc. Chem. Res.* **2015**, *48*, 1601-1611.